

# **Statistical Assessment of Aqua-MODIS Aerosol Optical Depth over Coastal Regions: Bias Characteristics, Empirical Corrections, and Sediment Effects**

**Jacob C. Anderson<sup>1</sup>, Jun Wang<sup>1,\*</sup>, Jing Zeng<sup>1</sup>, Maksym Petrenko<sup>2,3</sup>,**

**Gregory G. Leptoukh<sup>2,\*\*</sup>, Charles Ichoku<sup>2</sup>**

<sup>1</sup>Department of Earth and Atmospheric Science, University of Nebraska-Lincoln, Lincoln, NE.

<sup>2</sup>NASA Goddard Space Flight Center, Greenbelt, MD.

<sup>3</sup>Earth System Science Interdisciplinary Center, University of Maryland, College Park, MD.

\*Corresponding Contact:

Jun Wang: [jwang7@unl.edu](mailto:jwang7@unl.edu)

303 Bessey Hall

Lincoln, NE, 68588

\*\*Deceased January 2012.

Submitted to

*Atmospheric Measurement Techniques*

July 2012

Revised

November 2012

## Abstract

Coastal regions around the globe are a major source for anthropogenic aerosols in the atmosphere, but the underlying surface characteristics may not be favorable for the Moderate Resolution Imaging Spectroradiometer (MODIS) algorithms designed for retrieval of aerosols over dark land or open ocean surfaces. Using data collected from 62 coastal stations worldwide from the Aerosol Robotic Network (AERONET) in 2002-2011, statistical assessments of uncertainty are conducted for coastal aerosol optical depth (AOD) retrieved from MODIS aboard Aqua satellite, from the Collection 5.1 dataset. It is found that coastal AODs (at 550 nm) characterized respectively by the 'Dark Target' Land algorithm and Ocean algorithm all exhibit a log-normal distribution, which contrasts to the near-normal distribution of their corresponding biases. After filtering by quality flags, the MODIS coastal AODs from both the Land and Ocean algorithms are highly correlated with AERONET AODs (with  $R^2 \approx 0.8$ ), but only fall within the expected error envelope greater than 66% of the time for the Land algorithm. Furthermore, the MODIS AODs show statistically significant discrepancies from their respective counterparts of AERONET in terms of mean and frequency. Overall, the MODIS Ocean algorithm overestimates the AERONET coastal AOD by 0.021 for  $AOD < 0.25$  and underestimates it by 0.029 for  $AOD > 0.25$ . This dichotomy is shown to be related to the ocean surface wind speed and cloud contamination effects on the satellite aerosol retrieval. Consequently, an empirical scheme is formulated that uses cloud fraction and the sea surface wind speed from Modern Era Retrospective-Analysis for Research and Applications (MERRA) for correcting the bias of AOD retrieved from the MODIS Ocean algorithm, and is shown to be effective over the majority of the coastal AERONET stations to (a) simultaneously reduce both the mean and the spread of the bias, and (b) improve the trend analysis of AOD. Further correlation analysis performed after the bias correction using reflectances retrieved by the independent MODIS Ocean Color algorithm shows that the MODIS AOD is also impacted by the concentration of pigments and suspended particulate matter in the coastal waters. While different applications of MODIS AOD in climate and air quality studies have their own tolerances of uncertainty, it is recommended that an improved treatment of sea surface wind and sediment over the coastal waters be an integral part in the continuous evolution of the MODIS AOD retrieval algorithm.

## 1. Introduction

Aerosols play an important role in the Earth's energy balance and hydrological cycle (Charlson et al., 1992) through scattering and absorbing radiation (direct affect), as well as by influencing cloud radiative effects through the modification of their microphysical properties in the atmosphere (indirect affect). These airborne particles also reduce visibility and affect human health (Samet et al., 2000). The Intergovernmental Panel on Climate Change (IPCC) in their fourth assessment reports that the aerosol direct and indirect effects can render a cooling powerful enough to offset the warming from the anthropogenic CO<sub>2</sub> by almost one-third (IPCC, 2007). However, this estimate is considered to have the largest uncertainties in the climate models, and a further reduction of such large uncertainties requires observation-based characterization of aerosol properties on a global scale (IPCC, 2007). One key aerosol property that satellite remote sensing has been providing globally and used widely by the research community in the last decade is the Aerosol Optical Depth (AOD), a parameter that can be considered as the first-order indicator of columnar aerosol mass and aerosol forcing (Remer et al., 2005). Hence, the quantitative description of AOD uncertainty characteristics is critical for an improved understanding of aerosol impact on the climate (IPCC, 2007), as well as for monitoring the surface particulate matter air quality (Hoff and Christopher, 2009).

Various studies have found that the uncertainties in the instantaneous AOD retrievals from satellite sensors such as MISR and MODIS are generally within the (pre-launch) expected error (EE) envelope that is often characterized as a linear function of AOD itself. For example, in comparison with world-wide AOD measured from AERONET, MODIS AOD product is shown to have an EE envelope of  $\pm(0.05 + 0.15 \cdot \text{AOD}_{\text{aeronet}})$  over the land and  $\pm(0.03 + 0.05 \cdot \text{AOD}_{\text{aeronet}})$  over the ocean (Levy et al., 2007a & 2010; Remer et al., 2005; Kahn et al., 2011, 2005). Since

these equations parameterize the retrieval uncertainty as a function of  $AOD_{aeronet}$ , their applicability for most AODs retrievals from satellites are constrained by the very limited spatial coverage of AERONET, although in practice many studies have used AOD retrieval value itself in these equations to infer its corresponding uncertainty (Yu et al., 2006; and references therein). Furthermore, such estimate of EE envelope is based upon the MODIS-AERONET AOD comparison over the whole globe. Therefore, it does not reflect variation of retrieval uncertainties due to the change of land surface type and atmospheric conditions (Hyer et al., 2011), nor does it contain any information related to the mean and the spread of the AOD biases (i.e., probability density function or PDF of bias). At regional scales such as over the semi-arid western U.S. or over the east Asia during Spring dust season, the mean bias of MODIS AOD is shown to be positive, and the AOD error is larger and often outside of the global EE envelope (Wang et al., 2010; Drury et al., 2008). It is further noted that assessment of PDFs of AODs and AOD bias is highly relevant to questions related to the reliability of representing extreme AOD events in satellite-based AOD climatology and/or air quality applications. Consequently, the characteristics of satellite-based AOD uncertainty cannot be fully revealed without an analysis at the regional scale and a characterization beyond the uncertainty envelope to include more statistical parameters (such as PDF of biases).

This study focuses on the characterization of MODIS AOD uncertainty over the coastal regions because: (a) MODIS AOD product over the coastal region is a simple union of the retrievals from algorithms that are designed for either over land only or over open-ocean only, and (as discussed below) neither algorithm has a dedicated scheme to characterize the surface reflectance at the coast that is often influenced by a sand-water mixture and water-leaving radiance contributed by the underlying sea shore and suspended matter in shallow ocean water;

(b) over half the world's population resides in the coastal region (Tibbetts, 2002), which makes assessment of the MODIS AOD product over the coastal region critical for understanding the global trend of AOD, especially the anthropogenic AOD.

Only AODs retrieved by the MODIS dark surface algorithms, i.e., the MODIS Ocean (hereafter Ocean) algorithm and the MODIS Dark Target (hereafter Land) algorithm are evaluated in this study. Both the Ocean and Land algorithms use the cloud-free Top Of the Atmosphere (TOA) reflectances that are measured at resolutions ranging from 250 m in the shortwave visible wavelengths to 500 m in the near-infrared and are then aggregated to boxes of 20 by 20 (500 m resolution) pixels or equivalent to 10 by 10 km resolution at nadir for aerosol retrieval (Remer et al., 2005). The Ocean algorithm is used for retrieval if all pixels within the 20×20-pixel box are water; otherwise, the Land algorithm is used. Determining if a pixel is over land or over water is based upon the MOD35 1-km data that contains information about surface type (Remer et al., 2005). To date, a simple union of the AODs retrieved from the Land and Ocean algorithms make up the MODIS, level 2, "Land\_And\_Ocean" AOD product that is popularly used in the research community. However, within a repeat cycle of 16 days, a box of MODIS 20 by 20 pixels over the coast can be exactly equal to 10 by 10 km<sup>2</sup> (of ocean surface) when viewed by MODIS at nadir, but can also be equivalent to 20 by 48 km<sup>2</sup> area when viewed by MODIS at the high viewing zenith angle. In the first (nadir) case, the Ocean algorithm can be applicable; but in the latter case, the 20 by 20 pixels can possibly contain one or more land pixel(s), and the Land algorithm has to be applied. Consequently, assessment of MODIS AODs retrieved over the coast differs from the assessment in other regions because it requires evaluation to be conducted separately for Land and Ocean algorithms but likely with the same set of AERONET data along the coast.

In addition, to examine the relative performance of Ocean and Land algorithm along the coast, this study will also look into the assumptions made by the MODIS Ocean algorithm related to specification of the water-leaving radiance and the configuration of rough ocean surface model that computes sun glint patterns and reflectance due to white caps (Kleidman et al., 2012). The spectral water-leaving radiances are contributed by suspended material in the water and shallow ocean floor, and can vary significantly from open-ocean to coastal ocean. However, such variation is not considered in the current MODIS aerosol algorithm that assumes 0.0 water leaving radiances (due to sediments) for all but the 550 nm channel where a value of 0.005 is assumed (Remer et al., 2005). The impact of this assumption on MODIS AOD retrievals will be studied here by relating the MODIS AOD bias with respect to the water leaving radiances retrieved independently from MODIS ocean-color algorithms.

The sun glint pattern and the reflectance contribution from the white caps are both estimated in the Ocean algorithm with a Cox and Munk (1954) rough ocean surface model assuming a constant  $6 \text{ m s}^{-1}$  wind speed (Tanre et al., 1997). This assumption is shown to lead to retrieval errors over the open oceans (Kleidman et al., 2012), and an empirical method for correcting AOD errors due to this assumption and cloud contamination has been proposed (Shi et al. 2011; Zhang and Reid 2006), primarily for the purpose of data assimilation of AOD over the open ocean. While this empirical method is shown to be effective to reduce the RMSE in the MODIS-AERONET AOD comparisons, two questions remain: (a) the extent to which such correction reduces both the mean and the spread of the MODIS AOD biases, and (b) the implication of such correction to the trend analysis of AOD. (a) is noted because the mean bias can be reduced while the spread of biases can be kept unchanged, increased or decreased, and an ideal correction method should reduce the spread of the bias as well. (b) is important because AOD trend over the

open ocean reported by past studies differ in sign (Hsu et al., 2012; Mishchenko and Geogdzhayev, 2007; Remer et al., 2008; Zhang and Reid, 2007; Zhao et al., 2011).

Reconciliation of such difference requires a full investigation of biases (as a function of time) for global AODs as well as the differences in sensor calibration and trend analysis techniques, and is out of the scope of this study. Nevertheless, Zhang and Reid (2010) showed that correction of cloud and wind effect on AOD has little impact on the trend of global mean of AOD. A similar topic is revisited here but over AERONET stations, and we demonstrate that our empirical correction method indeed has impacts on the AOD trend analysis.

To avoid the issues related to MODIS/Terra calibration (Levy et al., 2010), we here only evaluate the uncertainty of MODIS/Aqua AOD. We introduce the data used in this study in Section 2, evaluate the performance of the MODIS Ocean and Land aerosol algorithms over coastal regions in Section 3, present the analysis of water leaving radiance, sea surface wind, and cloud impact the MODIS Land\_And\_Ocean data set in Section 4, discuss the impact of the empirical correction on trend analysis in Section 5, and finally summarize the findings in Section 6.

## **2. Data Description, Collocation, and Classification for AERONET Coastal Sites**

An overview of the data products used for this research is provided in the first part of this section, including the MODIS aerosol algorithms and AOD product, AERONET aerosol measurements, sea surface wind speed, and MODIS normalized water-leaving radiance datasets retrieved from the MODIS ocean color algorithm. This is followed by the discussion of the processes used for collocating MODIS and AERONET AOD.

## 2.1 MODIS and AERONET AOD products

MODIS level 2, collection 5.1 aerosol data from the 4<sup>th</sup> of July, 2002 through the 10<sup>th</sup> of January, 2011 are used. MODIS AOD is reported at 7 wavelengths (470 nm, 550 nm, 660 nm, 870 nm, 1200 nm, 1600 nm, 2100 nm) for the Ocean algorithm and 4 wavelengths (470 nm, 550 nm, 660 nm, 2100 nm) for the Land algorithm. The 550 nm wavelength is used for comparison with AERONET because it is consistent with the primary wavelength used by many climate and chemistry transport models (Kinne et al., 2005) as well as previous MODIS validation studies (Levy et al., 2007a, & 2010; Remer et al., 2005). Note that: (a) vegetated surfaces are not “dark” at the 550 nm wavelength and, therefore, the AOD at this wavelength over land is derived from the retrieved AODs at the 470 nm and 660 nm channels (Levy et al., 2010); (b) the MODIS Ocean product provides two AOD datasets, one from the inversion using the best-fitting aerosol model, and another from the average of inversions using several well-fitting models (ATBD-2006; found online at [http://modis-atmos.gsfc.nasa.gov/MOD04\\_L2/index.html](http://modis-atmos.gsfc.nasa.gov/MOD04_L2/index.html)); the latter is used for this research. The quality of each MODIS AOD retrieval is represented by its associated quality flags ranging from 3 (high confidence) to 0 (low or no confidence) (Levy et al., 2010). On a global scale, it has been shown that 66% of those AOD retrievals with quality flag 3 over land and 1, 2, or 3 over ocean have the EE envelopes respectively of  $\pm(0.05 + 0.15 \cdot \text{AOD}_{\text{aeronet}})$  over the land and  $\pm(0.03 + 0.05 \cdot \text{AOD}_{\text{aeronet}})$  over ocean. (Remer et al., 2005; Levy et al., 2010).

The Land\_And\_Ocean AOD datasets are generated from a union of AODs retrieved respectively from Land and Ocean algorithm. It is noted, however, that collection 5.1 has two different variable names for Land\_And\_Ocean AOD; one is the “Image\_Optical\_Depth\_Land\_And\_Ocean” that has no QA involved in its production, and another is “Optical\_Depth\_Land\_And\_Ocean” that requires quality flags  $> 0$  over land, and  $\geq 0$

over ocean (ATBD, 2006); the latter data variable is consequently used here. However, unlike the Land and Ocean AOD datasets, the combination product does not report QA flags.

AERONET AOD is derived from direct sun photometer measurements in some or all of the following seven different spectral bands centered at 340 nm, 380 nm, 440 nm, 500 nm, 670 nm, 940 nm, and 1020 nm (Holben et al., 1998). AERONET measures the extinction of direct beam solar radiation, and applies the Beer-Lambert-Bouguer law to determine AOD (Holben et al., 1998) with uncertainties on the order of 0.01-0.02 (Eck et al., 1999). Only quality assured, cloud screened, AERONET Level 2 data are used in this study to evaluate the MODIS aerosol product (Smirnov et al., 2000). To facilitate the comparison with MODIS, AERONET AOD measurements are interpolated to the 550 nm wavelength from multiple MODIS wavelengths using a quadratic fit on a log-log scale (Eck et al., 1999).

## **2.2 Sea Surface Wind Speed Data**

Sea surface wind data ( $u$  and  $v$  components of the wind at ~2 meters above the surface) is extracted from the Modern Era Retrospective-Analysis for Research and Applications (MERRA) meteorological database (tavgl\_2d\_flux\_Nx; <http://disc.sci.gsfc.nasa.gov/mdisc/>, downloaded March 2012). The data is at 1/2 degree latitude by 2/3 degree longitude resolution and is re-analyzed through the Goddard Earth Observing System-5 Data Assimilation System (GEOS-5 DAS) version 5.2.0 that includes a new set of physics packages for the atmospheric general circulation model (Rienecker et al., 2011). The wind-related inputs into the MERRA system include wind speed data from Radiosondes, Pilot Balloon (PIBAL) measured winds, MODIS, Geostationary Operational Environmental Satellites (GOES), Special Sensor Microwave/Imager (SSM/I), Tropical Rainfall Measuring Mission (TRMM) Microwave Imager (TMI), NASA's Quick Scatterometer (QuickSCAT) and others (Rienecker et al., 2011). MERRA has been found

to be one of the “best performing” reanalysis products for ocean surface turbulent flux and wind stress parameters (Brunke et al., 2011), and its near surface wind speeds is shown to have biases within  $0.5 \text{ ms}^{-1}$  (Kennedy et al., 2011).

### **2.3 MODIS Remote Sensing Reflectance (Rrs) Data for Ocean Surface**

Remote sensing reflectance data (Rrs) for ocean surface are acquired from the MOD18 water-leaving radiance product (Gordon and Clark, 1981), and span the same time period as the MODIS AOD data presented above. Only available over the ocean, Rrs is reported daily at 9 km resolution for ten different MODIS spectral bands centered at 412, 443, 469, 488, 531, 547, 555, 645, 667, 678 nm. For a given MODIS band, Rrs is defined as the ratio between the normalized water-leaving radiance (with respect to zenith) and the extraterrestrial solar irradiance in that band (Gordon and Clark, 1981). The normalized water-leaving radiance is approximately the radiance that would exit the ocean in the absence of atmosphere with the Sun at the zenith (Gordon, 1997). Hence, Rrs is not dependent on the Sun-viewing geometry, and is primarily regulated by the relative concentration of water, phytoplankton pigment, suspended particulate matter and dissolved organic matter (or yellow substances) at the top layer of ocean surface (Gordon and Clark, 1981; Gordon and Wang, 1994). Rrs (with a unit of  $\text{sr}^{-1}$ ) is a standard parameter that is used in many ocean-color algorithms for deriving the Chlorophyll concentration, pigment concentration, and suspended particulate matter (Gordon and Clark, 1981). The retrieval of Rrs is based upon the knowledge of bi-direction reflectance of ocean and the MODIS-measured TOA reflectance at two narrow ocean-color bands (748 nm and 870 nm). Under the assumption of zero ocean reflectance at these two bands, the retrieval algorithm first conducts the atmospheric correction at these two bands, and then extrapolates the retrieved AOD into other shorter wavelength bands for deriving Rrs (ATBD-1999, found on line at

[http://modis.gsfc.nasa.gov/data/atbd/atbd\\_mod17.pdf](http://modis.gsfc.nasa.gov/data/atbd/atbd_mod17.pdf)). Past analysis shows that Rse has an uncertainty less than  $\pm 0.002$ , i.e.,  $\pm 0.6\%$  of  $R_{rs443\text{ nm}}$  (ATBD-1999).

## **2.4 MODIS-AERONET Collocation and Coastal Site Classification**

The spatially and temporally collocated MODIS and AERONET data pairs spanning years 2002-2011 for the full record of MODIS/Aqua are acquired through the Multi-Sensor Aerosol Product Sampling System (MAPSS, <http://giovanni.gsfc.nasa.gov/mapss/>) (Ichoku et al., 2002; Petrenko et al., 2012). Two methods for MODIS-AERONET collocation are used in MAPSS. The first is the mean method in which AERONET measurements within  $\pm 30$  minutes of the MODIS overpass time are averaged and compared against MODIS AOD retrievals averaged within a 55 km diameter centered over the AERONET sites (Ichoku et al., 2002); also saved in this comparison is the mode of the quality flags associated with each AOD retrievals (Petrenko et al., 2012). The second is the central method in which the MODIS AOD retrieval closest to the AERONET site is paired with the AERONET measurement that is closest to the MODIS overpass time. A recent study by Petrenko et al. (2012) shows little difference between the central and mean methods in terms of their comparison statistics (such as correlation) with AERONET AOD. Therefore, to be consistent with previous research and also to increase data samples in the evaluation, the mean method is used for the remainder of this research.

Over the approximately 9-year (2002 – 2011) record of Aqua-MODIS and AERONET AOD pairs,  $\sim 26\%$  of the AERONET stations is found to have MODIS retrievals from both the Ocean and Land algorithms (which is consistent with Ichoku et al., 2002), and consequently those sites are designated as coastal. However, only sites that have at least 15 high quality (QA flag 3 for Land and flags 1, 2, or 3 for Ocean) MODIS AOD retrievals, from both the Land and Ocean algorithms, during collocated AERONET AOD measurements are incorporated into this

analysis. Coastal sites range from approximately 13 km offshore (Venise AERONET site) to 15 km inland (Lecce\_University AERONET site). All other AERONET sites are designated as non-coastal, being either Land only or Ocean only.

### **3. Overall Performance of MODIS AOD in Coastal vs. Non-Coastal Regions**

The MODIS-AERONET AOD pairs are examined on a global scale and split into three categories. The first includes all AERONET sites (global), the second consists of only coastal AERONET sites (coastal), and the third is made up of only non-coastal sites (non-coastal). We utilize multiple metrics to statistically evaluate the MODIS AOD uncertainty with respect to AOD measured by AERONET.

#### **3.1 Metrics for Comparing MODIS and AERONET AOD**

The first type of metrics is a combination of parameters that are commonly used to describe the relationship between two variables including: bias, mean, standard deviation, correlation, statistical significance, and best-fit (ordinary-least-square) regressions. MODIS AOD bias is calculated by subtracting AERONET AOD from the paired MODIS AOD (respectively for Land, Ocean and Land\_And\_Ocean products). The mean bias is calculated by averaging the bias at each AERONET site for the full time period ~ 2002 - 2011. Furthermore, the correlation, variance and root mean square difference (RMSD) between MODIS AOD and AERONET AOD are combined to generate the well known Taylor Diagram to aid the visualization of the differences found in the comparison. The Taylor Diagram uses a 2D polar plot to demonstrate three pieces of information that are interconnected, in which radius represents normalized standard deviations, polar angle represents correlation, and the radius of the circles centered on point “REF” (e.g., radius of 1) along the x-axis indicates normalized RMSD. As will be shown in the next section, the Taylor Diagram is particularly useful for

visualizing the error characteristics of each of the MODIS aerosol algorithms over varying surface types.

While the first type of metric is useful, it is primarily based upon ordinary least square (OLS) regressions that is presented here to be consistent with previous research. However, OLS may not be the most appropriate technique for evaluating MODIS uncertainty with respect to AERONET, and the statistics from it may not be sufficient to fully describe the goodness of fit between two data sets, especially when the population in the datasets are not normally distributed (Wilks, 2011). The AOD frequencies over coastal sites (and non-coastal sites, not shown) are not normally distributed (Figure 1), and are indeed log-normal (Figure 2), which is consistent with previous studies (O'Neill et al., 2000). Two parameters,  $\mu$  and  $\sigma$ , represent respectively the mean and standard deviation of the logarithm of AODs, are identified and shown in Figure 2 to fully describe a log-normal PDF. The actual frequency for AOD values between  $\tau$  and  $\tau + \Delta\tau$  can be obtained by integrating the PDF over the range  $\tau$  to  $\tau + \Delta\tau$ , and then multiplying the integral by the total number of sample data points. Note that approximately 400 MODIS AOD retrievals (out of 46,548 retrievals paired with AERONET over the coastal regions) is found to have negative AOD values; those retrievals are not physical and are excluded in the fit of a log-normal distribution, but are included in other analyses (for bias, correlation, standard deviation, and RMSD) as recommend in Remer et al. (2005). Using a  $\chi^2$  test we find that the log-normal PDFs fit each AOD distribution at a statistically significant level (Figure 2). Because of the log-normal PDF of AODs, the high correlation and/or small bias, even at the statistically significant level, does not necessarily warrant that the fit between the PDF of AERONET and MODIS AODs is statistically significant.

To evaluate if the (log-normal) PDFs of MODIS AOD data fit with that of the AERONET measurements at the statistically significant level, a second type of statistic metrics is used that consists of a t-test for difference of mean for paired data, a likelihood ratio test, and a Kolmogorov-Smirnov (K-S) test. In the t-test for difference of mean for paired data, statistical significance is then applied to

$$z = \frac{\bar{\Delta} - \mu_{\Delta}}{\left(\frac{s_{\Delta}^2}{n}\right)^{\frac{1}{2}}}$$

, where  $\bar{\Delta}$  is the mean bias,  $\mu_{\Delta}$  is the difference between the means for each variable (e.g. MODIS AOD or AERONET AOD), and  $s_{\Delta}^2$  is the sample variance of the bias for a total of  $n$  pairs (Wilks, 2011). A very small p-value (less than 0.01) indicates at which statistically significant level (99%) that the null hypothesis is not true, or the difference between means for the paired data is significant.

A likelihood ratio test is a parametric test to determine the likelihood that the MODIS AODs could have been drawn from the same log-normal distribution as the AERONET AODs. To perform this test it is necessary to fit log-normal distributions separately to each MODIS algorithm and AERONET, and compare these two distributions with the single log-normal distribution fit using both sets of data (Wilks, 2011). The general form of the likelihood test statistic is

$$\varphi^* = 2 \cdot \ln \left[ \frac{\varphi(H_A)}{\varphi(H_0)} \right] = 2 \cdot [L(H_A) - L(H_0)]$$

, where  $\varphi(H_A)$  and  $\varphi(H_0)$  are the likelihood functions and  $L$  is the log-likelihood. For our case the test statistic is equal to

$$\varphi^* = 2 \cdot \left\{ \left[ \sum_{i=0}^{\tau} PDF_{MODIS} \right] + \left[ \sum_{i=0}^{\tau} PDF_{AERONET} \right] + \left[ \sum_{i=0}^{\tau} PDF_{MODIS \text{ and } AERONET} \right] \right\}$$

where the PDFs are a function of  $\mu$ ,  $\sigma$ , and  $\tau$ . Since there are 4 parameters used to estimate the individual AERONET and MODIS distributions and 2 for the null hypothesis that MODIS and AERONET AOD data are from the same PDF ( $PDF_{MODIS \text{ and } AERONET}$ ),  $\varphi^*$  is evaluated with the  $\chi^2$  table for degrees of freedom (of  $v=2$ ).

Since likelihood test only evaluates the goodness of fit among log-normal PDFs that itself is an approximation to the actual PDF, the K-S test is used to further compare the cumulative distribution functions (CDFs) of each of the MODIS algorithms to that of AERONET. The test statistic is represented by the maximum difference between the MODIS and AERONET CDFs

$$D = \max|CDF_{MODIS} - CDF_{AERONET}|$$

. When  $D$  is greater than the critical value,  $1.36/\sqrt{n}$ , the null hypothesis (the two CDFs show a good fit) is rejected at the 99% confidence level. By analyzing the fit between the MODIS and AERONET PDFs and CDFs, our evaluation goes beyond the bias and correlation tests that have been used commonly in the past to evaluate MODIS AOD uncertainty, and hence provides a more robust statistical assessment and a more complete description of the uncertainties in MODIS AOD retrievals.

### **3.2 Coastal vs. Non-Coastal MODIS AOD Evaluation**

As mentioned in Section 2, the Land\_And\_Ocean AOD product doesn't have its own QA, and therefore, is filtered in this study using the MODIS science team's recommendations that retrievals originating from the Land algorithm have a flag equal to 3 and those originating from the Ocean algorithm has a flag greater than 0. This QA filtering is similar to what is used for the Land\_And\_Ocean AOD product, except that we use only land AOD with flag = 3 and ocean AOD with flag >0. Note that the mean AOD calculated from the Land\_And\_Ocean dataset may not be equal to the mean AOD calculated from the separate Land or Ocean datasets because

the mean of the Land\_And\_Ocean product, within the 55 km region around AERONET, may include MODIS pixels originating from either (or both) the Ocean and Land algorithms.

After quality flag filtering, MODIS AODs are highly correlated with the paired AODs from AERONET with  $R^2$  greater than 0.8 regardless of whether AODs are retrieved over coastal or non-coastal region (respectively shown in top and bottom row in Figure 3, Table 3).  $R^2$  for the Ocean AOD, Land AOD, and Land\_And\_Ocean AOD products are also greater than 0.8 (respectively shown in three columns in Fig. 3, Table 3). MODIS AOD retrievals from the Ocean algorithm on a global scale have  $R^2$  of 0.81 that is much less than the  $R^2$  of 0.85 for non-coastal open-ocean sites, but similar to the  $R^2$  of 0.80 for coastal sites (Table 3). In contrast, Table 3 shows that little change in correlation with AERONET AOD is found for AODs from the MODIS Land algorithms over the coastal ( $R^2$  of 0.795), non-coastal ( $R^2$  of 0.795), and global evaluations ( $R^2$  of 0.793). This contrast suggests room for improvement in the Ocean algorithm over coastal regions, which is further supported by the fact that the linear regression interception found for the Ocean algorithm is positive over coastal sites at 0.034, an order of magnitude larger than the counterpart for non-coastal sites at -0.001 (Table 3). However, consistent with past analyses (Kahn et al., 2011, 2007, 2005; Levy et al., 2007a, 2010; Mi et al., 2007; Remer et al., 2005; and others), the Ocean AOD correlations are greater than the Land AOD correlation in all (coastal, non-coastal, and global) categories (Table 3).

Figure 3 also shows that the AODs over coastal and non-coastal regions retrieved from the Land algorithm both fall within the expected uncertainty envelope greater than 66% of the time (Fig. 3b and 3e), but the counterparts from Ocean algorithm only fall within the EE envelope ~58% of time, which is lower than 66% that is revealed from the past studies of MODIS *collection 4* that don't separate the AERONET-MODIS AOD comparisons into coastal

and non-coastal regions (Remer et al., 2005). Nevertheless, since the uncertainty envelope for Ocean algorithm is smaller than that for Land algorithm, its bias is found to be less (Figure 3).

While a small bias (often  $< 0.03$ , Figure 3) of AOD overall is consistent with past research (Levy et al., 2010; Remer et al., 2005), for the same type of product (e.g., from Ocean algorithm, Land algorithm, and combined Land\_And\_Ocean), a larger bias of AOD is apparent over the coastal regions than over non-coastal regions (Fig. 3d-3df). It is noted that for AOD from the Ocean algorithm, the overall bias (0.012) along the coast is larger than the counterparts (0.006) over the open ocean (Fig. 3f vs. 3c). This is indeed misleading because of two counteracting effects over the coast where AOD larger than 0.25 are underestimated by 0.029, whereas those smaller than 0.25 are overestimated by 0.021 (Table 1). Using a t-test for difference we find that regardless of the MODIS product (i.e., Ocean, Land, Land\_And\_Ocean), the AOD bias over coastal regions are statistically significant with a p-value much less than 0.01.

It is also interesting to find that the PDF of bias, regardless for Ocean algorithm, Land algorithm, and Land\_And\_Ocean product, all show the normal distribution (Figure 4). The contrast between the log-normal PDF of AOD and the normal PDF of AOD bias suggests that the actual bias of MODIS instantaneous AOD is not a simple linear function of AOD as indicated in the EE envelope. This can be understood because: (a) large AOD sometimes have large signal for and result in less uncertainty in the retrieval; and (b) many other factors (other than AOD) such as viewing geometry and boundary conditions can complicate the retrieval uncertainty.

In order to gain insight into the locality of the bias, a plot of bias at different coastal stations is shown in Figure 5. AODs retrieved from the Land algorithm are shown to have a significantly larger bias than the Ocean algorithm for most coastal AERONET sites. This is

expected because of the inherent difficulties in characterizing land surfaces in general. The average MODIS AOD bias for the Land algorithm over coastal sites is 0.026 at the statistically significant level ( $p < 0.01$ ) and shows little dependence on AOD amount (Table 1). However, the bias does show large variation amongst different coastal AERONET sites (Figure 5), likely reflecting the high variation of surface characteristics along the global coast.

The Taylor Diagram (Figure 6) visualizes the overall performance of different sets of MODIS AOD data in a single figure. The MODIS-AERONET AOD correlation coefficient visibly decreases for coastal retrievals compared to non-coastal retrievals, especially from the Ocean algorithm (Figure 6). Furthermore, the normalized standard deviations of MODIS AOD increase from  $\sim 0.8$  for non-coastal retrievals to 1.3 for coastal retrievals (Figure 6), indicating that MODIS AOD is less capable of capturing the temporal variation of AERONET AOD over the coastal sites. By the same token, Figure 6 also demonstrates that the Ocean algorithm over the open-ocean (non-coastal) captures the variation in AOD better than the other algorithms, because its resultant representation in the Taylor diagram is closest to the point “REF” indicating the best performance with respect to AERONET. It is shown that all of the MODIS AOD retrievals over the coast, regardless of algorithm, cluster farthest away from the “REF” point, indicating a need for refinement of the MODIS product over coastal regions (Figure 6).

To further evaluate if MODIS aerosol products represent the climatology observed from AERONET, the PDFs from the MODIS products are used to compare against the PDF from AERONET. The likelihood test returns a test statistic  $\phi$  as described in Section 3.1. The test statistic is compared to a critical value to determine the likelihood that the MODIS AOD PDF fits the PDF from AERONET AOD. The critical value for the  $\chi^2$  statistics with  $v=2$  degrees of freedom at the 99% confidence level is 9.210, where anything greater than this value results in

rejection of the null hypothesis that the PDFs may come from the same distribution. We find that the test statistics are 23.03, 29.77, and 22.98 for the quality filtered MODIS Land, Ocean, and Land\_And\_Ocean products, respectively. Hence, the PDFs from the MODIS algorithms statistically differ from the PDFs of AERONET AOD over coastal regions. This finding suggests that from a mathematical point of view, MODIS AOD statistics may not fully represent the nature of AOD climatology described by AERONET, although the implications of such finding to the real applications in climate studies depends on how much uncertainty these applications can tolerate. The likelihood test is useful to compare PDFs that is parameterized to fit the observation data, but the not the actual histogram of MODIS AOD. To more fully describe the fit between MODIS and AERONET data, our analysis is extended to actual CDFs as well.

Figure 7 displays the results of the K-S test and maximum difference for the CDFs from each quality filtered MODIS algorithms with respect to the CDF from AERONET. The critical values (described in Section 3.1) needed to accept that the MODIS Land, Ocean, and Land\_And\_Ocean AOD CDFs fit the counterpart of the AERONET AOD, at a 99% confidence level, are respectively 0.013, 0.009, and 0.008 (Figure 7). It is clear in Figure 7 that the maximum departures of the CDFs from each of the MODIS AOD products and AERONET AOD observation are greater than the corresponding critical values (Figure 7). Hence, the null hypothesis (i.e., CDFs from MODIS AODs and AERONET AODs are drawn from the same data population) must be rejected and the CDFs from each of the MODIS algorithms diff the AERONET CDF at the 99% confidence level. This finding only strengthens conclusion from the previous tests that MODIS AOD PDF statistically differ from AERONET counterpart, although it should be reiterated that implications of such findings to real applications depend on how much uncertainty these applications can tolerate.

### 3.3 Impact of QA filtering on Land\_And\_Ocean AOD

For completeness, the effect of QA filtering on the analysis is presented here. The filtering criteria recommended by the MODIS team improves the global MODIS Land\_And\_Ocean correlation ( $R^2$ ) with AERONET from .74 to .80 (Table 3), and reduces the AOD bias by 34% for coastal regions from 0.029 to 0.019 (Table 1). Focusing on the high AOD events ( $AOD > 0.25$ ) over the coast, the bias is reduced even more (by 62%) from 0.026 to 0.010 (Table 1). However, as a result of filtering, the number of MODIS-AERONET AOD pairs is reduced from 113,152 to 71,303 globally (or by 37%). The Land\_And\_Ocean, quality filtered, data set has a regression equation of  $\tau_M = 0.964 \cdot \tau_A + 0.014$  on a global scale over the full record of MODIS (Table 3), and  $\tau_M = 0.933 \cdot \tau_A + 0.028$  over coastal regions (Figure 3). The reduction in bias from the quality filtering can be further observed in Figure 5d vs. 5e and an increase in correlation is found on a global scale. However, as discussed in previous section, even after the quality flag filter, the coastal regions still show poorer MODIS performance compared to the non-coastal retrievals. The result suggests that a dedicated algorithm for coastal retrievals may be needed in lieu of the current Land and Ocean algorithms used for MODIS aerosol retrievals. It is noted that the release of MODIS collection 6, the Optical\_Depth\_Land\_And\_Ocean data will be created by applying the same AQ filtering technique as used in this study (as also recommended by the MODIS aerosol science team) rather than the current removal of AOD retrievals with zero flag in Collection 5.

### 4. Wind, Cloud, and Water-leaving radiance Impact on the MODIS Ocean Algorithm

Different sources of error arise in the MODIS Ocean retrievals because of surface characteristic assumptions made by the algorithm, and the uncertainty in the cloud-mask algorithm designed specifically for the MODIS Ocean product to classify a pixel as cloud free.

We examine the impact of the sources of error separately on the MODIS performance over the coastal regions. We expand the cloud contamination and near surface wind speed analysis that was conducted by Shi et al., (2011) primary over global oceans to focus on the coastal retrievals, and add new analysis to reveal the impact of water-leaving radiance contributed by the pigments and suspended particulate matter in the coastal water on the MODIS AOD retrieval.

#### **4.1 Cloud Impact**

Using the AEROENT AOD that is spatially paired with MODIS AOD at the pixel level (i.e., the central method in MAPSS), past studies showed the impact of cloud contamination in the MODIS AOD retrievals over the ocean (Zhang and Reid, 2006; Shi et al., 2011). The similar investigations are conducted here for the *collection 5.1* MODIS product, but focusing on coastal AERONET stations only and analyzing the statistics based upon the AERONET-MODIS paired AODs and the mean cloud fraction that are in turn created with the mean method from MAPSS. Multiple thresholds (80%, 70%, and standard QA flag) for cloud fraction above which the AOD will be considered to have larger error and should be filtered out in the analysis, are tested, and the corresponding results are given in Table 2. The analysis reveals that the 70% threshold can greatly reduce bias while maintaining a sufficient number of retrievals, with a reduction of only 16% globally and 14% over coastal regions (Table 2). For the cloud fraction threshold of 70% (80%) the reduction of bias for coastal sites is 100% (67%) and for non-coastal sites is 58% (33%) (Table 2).

While Table 2 shows consistent results with Zhang and Reid (2006) and Shi et al. (2011) that the removal of MODIS over-ocean AODs associated with a cloud fraction larger than a threshold of 80% can significantly reduce the bias in AOD estimates, a more detailed examination also shows that the cloud fraction filter leads to an even more negative bias for

AODs over 0.25 and reduces the positive bias for AOD less than 0.25 (Table 2). Zhang and Reid (2006, 2010) demonstrate that the cloud contamination causes MODIS overestimation due to the high reflectivity of clouds in the visible spectrum, and therefore, filtering AOD retrievals by cloud fraction would lead to an overall decrease in MODIS AOD. The same physical interpretation is true for MODIS collection 5.1. However, the negative bias persistence for AOD over 0.25 requires another explanation. A possible cause of the more negative bias (AOD > 0.25) after cloud filtering (Table 2) is that cloud contamination has a greater influence, proportionally, on lower AOD retrievals than on higher AODs (Kleidman et al., 2012). Thus, the cloud contamination filter removes some of the high AOD events that are minimally impacted by high cloud fractions, and may skew the results to a more negative bias. This impact needs to be evaluated in future studies.

## **4.2 Wind Speed Impact**

In addition to cloud contamination, past studies also showed a systematic increase of MODIS error as a function of wind speed for retrievals over the open-ocean. This dependence is most apparent when wind speed deviates from the  $6 \text{ m s}^{-1}$  speed assumed for the rough ocean surface and white cap parameterizations within the MODIS Ocean algorithm (Zhang and Reid, 2010; Shi et al., 2011; Kleidman et al., 2012). Previous work on wind climatologies suggests that surface wind speeds over coastal regions are frequently slower than  $6 \text{ m s}^{-1}$  (Lavagnini et al., 2005; Martin et al., 1999). To quantify the impact of the surface wind speed on coastal aerosol retrievals, we stratify the analysis of MODIS-AERONET biases (before and after cloud-contamination filtering) as a function of ocean surface wind speed. At every coastal AERONET site, each MODIS AOD bias is paired spatially and temporally with the corresponding 2-meter wind speed from the MERRA re-analysis.

Shown in Figure 8 is a linear best fit of  $\tau_{\text{bias}} = 0.010 \cdot v - 0.020$  before cloud filtering, where  $\tau_{\text{bias}}$  is MODIS AOD bias and  $v$  is wind speed. The positive correlation between bias and wind speed is consistent with previous work (Zhang and Reid, 2010; Shi et al., 2011; Kleidman et al., 2012) and can be quantitatively understood from the following two factors: (1) wind speeds over coastal regions are frequently (94% of the time) less than  $6 \text{ ms}^{-1}$  MODIS overpass time (Figure 8b), and (2) slower wind speeds lead to more negative MODIS bias while faster wind speeds lead to positive bias (Figure 8a). While factor (1) explains, in part, the negative bias for the AOD (greater than 0.25) retrieved from the Ocean algorithm, factor (2) can be used to interpret the overestimation in MODIS AOD for AOD less than 0.25 over the coast. High AOD near the coast may occur during high wind conditions that can generate more sea salt particles or may be associated with frontal passage moving aerosols; in either case, such high winds can lead to error in MODIS AOD retrievals. This effect on MODIS retrievals needs to be studied in future research. However, with the known impact of cloud contamination, we conduct a similar analysis after filtering out the MODIS AOD retrievals with cloud fractions greater than 70%, and found that  $\tau_{\text{bias}} = 0.010 \cdot v - 0.024$  (Figure 8c).

Geographically, a statistically significant correlation between MODIS AOD bias and wind speed is found at 46 out of total 62 coastal AERONET sites (Figure 9a). From those statistically significant sites, 40 are found to have a negative MODIS bias as the wind speed approaches zero (Figure 9c), and 45 are found to have a regression with a positive slope that indicates a systematic positive bias in MODIS AOD as wind speeds increase (Figure 9d). Those 16 AERONET sites that do not show a statistically significant correlation between MODIS bias and wind speed have two main characteristics in common: 1) the MODIS AOD correlation with AERONET AOD is less than the average correlation for the coastal group; 2) all of the

AERONET sites are close to the coastline (i.e. within 5 km) except Bac\_Lieu which is ~8.5 km from the coastline. (1) suggests that the retrieval errors at these sites are not systematic, and (2) indicate that the rough ocean surface model may not be appropriate to estimate the surface reflectance in the first place, which is supported by the analysis in the following section.

### **4.3 Bias Correction for Wind Speed and Cloud**

Zhang and Reid (2006) showed that empirical correction of wind and cloud effect can reduce the absolute bias in the MODIS AOD product. To further evaluate the empirical correction on the MODIS AOD uncertainty characteristics, we study the change of mean and PDF of MODIS AOD bias before and after the correction. Because the wind speed and cloud fraction are not correlated (Figure 8d), a correction scheme that accounts for each independently, is applied to MODIS QA-filtered AOD. By including the MERRA wind speed at approximately the time of each MODIS AOD retrieval, the MODIS AOD bias is estimated from regression equation,  $\tau_{\text{bias}} = 0.010 \cdot v - 0.024$  found in Section 4.2 (after filtering AODs with 70% or more cloud fraction) and is subsequently subtracted from the corresponding AOD to create an empirically corrected AOD.

A reduction in overall MODIS AOD bias for the Ocean algorithm over the coast is found, with a change of mean bias of +0.011 for the standard quality flag filtered MODIS product to -0.0005 for the cloud and wind corrected AOD (Figure 4). Furthermore, for AOD events less than 0.25 the bias is reduced from +0.021 to +0.0098, and for AOD events greater than 0.25 the bias is reduced from -0.029 to -0.027 (Figure 4). In addition, the empirical correction reduces spread (or geometric standard deviation) of bias in Land\_And\_Ocean product from 0.074 to 0.067 (Figure 4d). As a result of reducing mean and spread of the bias after empirical correction, it is evident in the Taylor diagram that the empirical corrections improve the MODIS AOD

correlation with AERONET and reduce the variance in observation, indicating that the temporal variation of AERONET AOD is better captured by the corrected product. Furthermore, after both cloud and wind correction the MODIS frequency shows a better fit to the AERONET distribution than the standard MODIS Ocean product (Figure 10). Although the corrected MODIS AOD CDF does not pass the K-S test with a maximum difference of 0.024 and a critical value of 0.011, at the 99% confidence level, the correction does show an improvement by reducing the maximum difference between the AERONET CDF and the standard MODIS product (Figure 10).

#### **4.4 Impact of Sediments on the Residual Bias**

Finally, the effectiveness of using a rough ocean surface model (designed for open ocean or case 1 water) to model the surface reflectance at the coastal (case-2) water is evaluated. In MODIS Ocean algorithm, a sediment mask procedure is first applied before the retrieval is conducted. This procedure computes the expected top-of-atmosphere (TOA) reflectance at 550 nm based upon a power law fit from the TOA reflectances at 470, 1200, 1600, 2100 nm wavelengths, and any pixel with measured TOA reflectance at 550 nm larger than the expected counterpart by 0.01 is flagged as sediment-dominant pixel and is not included in the retrieval (Li et al., 2003). Furthermore, the MODIS Ocean algorithm assumes that water-leaving radiance contributed by the pigments is 0.005 at 550 nm and 0.0 at all other wavelengths (Remer et al., 2005).

Apparently, similar to any threshold-based method (such as for cloud screening), the fixed thresholds used in the sediment mask and the treatment of pigment contribution to the water-leaving radiance may result in retrieval biases. Gordon (1997) showed that the pigment concentration is inversely proportional to the  $R_{rs}$  ratio between light-blue and mid-visible

wavelengths because pigments have stronger absorption in shorter wavelengths. Miller and McKee (2004) found that the total suspended matter in the coastal waters is linearly and positively proportional to and hence can be derived from the MODIS (band 1) TOA reflectance at 645 nm. Consequently, analysis is conducted to correlate MODIS Ocean AOD bias (after the empirical correction in Section 4.3) respectively with  $\log_{10}(R_{rs443}/R_{rs550})$  and  $R_{rs645}$  (Figure 11).

Figure 11a reveals that the MODIS AOD bias linearly increases with both  $\log_{10}(R_{rs443}/R_{rs550})$  and  $R_{rs645}$  at the significant level with  $p < 0.1$ . This can be understood that the higher  $\log_{10}(R_{rs443}/R_{rs550})$ , the less is the pigment concentration and pigment absorption, and therefore the bias will be smaller. As expected, the intercept between the bias and  $\log_{10}(R_{rs443}/R_{rs550})$  should be negative because larger amount of pigment will reduce the water-leaving radiance, and without taking account of this reduction, an underestimation of AOD (or negative bias) can occur in the retrieval algorithm. Certainly, depending on the amount of pigment considered in the MODIS rough ocean model, any further departure from this amount will result in larger biases. However, since the bias is shown to be close to zero when  $\log_{10}(R_{rs443}/R_{rs550})$  is at the high end (Figure 11a), it suggests again that the rough ocean model used in MODIS aerosol algorithm is well suited for the retrieval over the open ocean.

Interestingly, the positive linear correlation is also found between the MODIS AOD bias and  $R_{rs645}$  (Figure 11b), but with nearly zero (0.001) intercept (in contrast to an intercept of -0.01 in the relationship between the bias and  $\log_{10}(R_{rs443}/R_{rs550})$ ). This can be explained by the fact that at 645 nm, suspended matter often increases the water-leaving radiance at the coastal water through their backscattering; without this correction of increase in the MODIS AOD retrieval algorithm, the resultant retrieval will have an overestimation (positive bias). The zero intercept nicely shows that the MODIS retrieval algorithm with the assumption of zero water-

leaving radiance due to the sediment works best for the open ocean. In coastal regions it is highly possible that some sediments are missed by the sediment mask algorithm developed by Li et al. (2003). Hence, the higher concentration of suspended matter (or Rrs), the more is the positive bias, which is shown in Figure 11b.

## **5 The Impact of Empirical Corrections on AOD Trend Analysis**

Quantification of the uncertainty in the AOD trend analysis can be challenging because of the effect of time autocorrelation in the datasets, the effect from large anomaly of general circulation (such as ENSO), and the aggregation of uncertainties in the instantaneous measurements in the temporal and spatial averages. While a thorough study of these issues is beyond the scope of this study, we demonstrate the importance of characterization and correcting the bias in the instantaneous AOD for the trend analysis. For this purpose, annual AOD trend is computed for each coastal AERONET station from the three data sets including AERONET AOD, MODIS QA-filtered AOD retrieved from Ocean algorithm (hereafter Ocean AOD), and MODIS QA-filtered empirically-corrected AOD retrieved from Ocean algorithm (hereafter corrected Ocean AOD). Similar to our past study of surface wind trend (Holt and Wang, 2012), the trend computed here is based upon the OLS regression with correction of time autocorrelation. Only those stations that have a minimum of 4 years of AERONET data are used in the trend analysis.

Overall, AERONET trends found in this study over the Eastern USA and Europe show a slightly decreasing AOD pattern around  $-0.005 \text{ AOD yr}^{-1}$ , which is comparable with Hsu et al. (2012). Two AERONET sites (“Dunkerque” at 51.035N and 2.368W, “Karachi” at 24.87N and 67.03E), whose AOD trends are representative of their corresponding regional AOD trend found in Hsu et al., 2012, are chosen to demonstrate the differences in the trends computed for MODIS

Ocean AOD and MODIS Ocean corrected AOD (Figure 12). At Dunkerque the annual AOD trends from AERONET, MODIS Ocean algorithm, and MODIS corrected are -0.005, -0.003, and -0.005, respectively. At Karachi the annual AOD trends from AERONET, MODIS Ocean algorithm, and MODIS corrected are -0.017, -0.007, and -0.016 (Figure 12).

Geographically (Figure 12), over the most (34 stations out of 46) AERONET stations, trends computed using MODIS AOD after empirical correction (TrendCorrected) fit more closely with their respective AERONET counterparts (TrendAERONET) than those without bias correction in MODIS AOD (or TrendNoCorrected). We quantify this improvement through two steps. First, the absolute departures of TrendAERONET and TrendNoCorrected with respect to TrendCorrected are both calculated. Second, the difference of these two departures is normalized to the absolute value of TrendNoCorrected; a positive value of this normalized ratio indicates an improvement due to bias correction, and a negative value means that the trend is further away from the trend computed with AERONET data. Overall, the relative improvements of more than 50% are apparent in many stations shown in Figure 12, while over the stations where the empirical correction makes trend calculation worse, the difference is less than 50%. Nevertheless, while further detailed analysis of the trend is out the scope of this study, Figure 12 demonstrate the importance of correcting bias in MODIS AOD for the analysis of AOD trend.

## **6 Conclusions and Discussion**

Aqua-MODIS AOD products retrieved during 9 years are evaluated using spatially and temporally collocated AERONET AOD data. Specific focus in the analysis is given to the coastal regions of the world due to their complex surface characteristics and their dominant contribution to the loading of anthropogenic aerosols in the atmosphere. Our findings can be summarized into the following points.

(a) Over the coast the MODIS aerosol algorithms show increased uncertainty with respect to non-coastal regions. After filtering by quality flags, the MODIS AODs respectively retrieved from the Land and Ocean algorithms are highly correlated with AERONET (with  $R^2 \approx 0.8$ ), but only the Land algorithm AODs fall within the expected error envelope greater than 66% of the time. Furthermore, quality flag filtered MODIS AODs, from all of the Land, Ocean, and Land\_And\_Ocean products, show statistically significant discrepancies with respect to their counterparts from AERONET in terms of both mean and frequency, suggesting the need for improvement in MODIS retrieval algorithms over the coast.

(b) Analysis clearly demonstrates that the MODIS Ocean algorithm has three error sources over coastal regions, respectively related to the cloud mask, assumption of sea surface wind speed, and treatment of the sediment contribution to the water-leaving radiance. The overestimate of AOD due to cloud contamination and the underestimation of AOD due to the use of constant  $6 \text{ ms}^{-1}$  wind speed, which are found over the coastal region, are in agreement with Zhang and Reid's (2006, 2010) global MODIS AOD analysis. Based upon MERRA data, we found that wind speeds over the coastal ocean are frequently lower than the  $6 \text{ ms}^{-1}$  assumed by the MODIS Ocean algorithm, which indicates that the surface reflectance is smaller than what is used in the Ocean algorithm for the coastal regions. After empirical correction of cloud and sea surface wind speed, the residual bias is found to be affected by the pigment and suspended particulate matter along the coastal water that are respectively characterized by the remote-sensing reflectance at different wavelengths. MODIS AOD has low bias during higher pigment conditions, and high bias when suspended matter in coastal water is higher. The analyses show that the sediment mask used in the MODIS algorithm is not likely sufficient to remove sediment

edges, and the assumption of zero contribution by suspended matter to the water-leaving radiance at longer wavelengths is not applicable to coastal waters.

(c) The bias for MODIS AOD before and after empirical correction is characterized beyond the mean bias. In contrast to the lognormal distribution of AOD, the MODIS AOD bias indeed has the normal distribution, which suggests that the instantaneous bias is not a simple linear function of MODIS AOD value itself. Empirical correction for cloud and sea surface wind speed reduces both the mean and spread of MODIS AOD bias, and is shown to have important implications for trend analysis.

It should be noted that while our analysis of retrieval error sources is based upon the physical reasoning and supported by the statistical results, the statistical significance is mainly evaluated from a mathematical point of view. Implication of these statistical results to the applications of AOD for climate studies or air quality monitoring should be interpreted with caution because each application has its own requirement of the data accuracy and tolerance of uncertainty. Nevertheless, a full characterization of MODIS AOD bias (including its mean and spread) as well as the analysis of retrieval error sources for the formulation of empirical correction schemes are both needed to reduce and quantify the uncertainty in the utility of MODIS AOD for climate and air quality studies. As MODIS retrieval algorithm evolves with continuous improvement, the framework to analyze its uncertainty should also evolve with continuous improvement toward full characterization of its bias statistics and error sources. It is recommended that treatment of sediment mask and contribution of sediments to the water-leaving radiances should be an integral part in the near future refinement of MODIS aerosol algorithm.

## **Acknowledgements**

Funding for this research was provided by NASA GSFC, NASA Nebraska Space Grant Consortium, and the Department of Earth and Atmospheric Sciences at the University of Nebraska-Lincoln. We would like to give a special thanks to Scott Mellor for helping edit the manuscript. J. Wang also acknowledges the NASA Radiation Science Program and Atmospheric Composition and Analysis Program for support. Our final thought is for Gregory Leptoukh who tragically passed away during this research. Without his vision and foresight this project would have never been possible.

## **References**

- ATBD, 2006: Algorithm for remote sensing of tropospheric aerosol from MODIS: Collection 5, Product ID: MOD04/MYD04. [Available online at [http://modis.gsfc.nasa.gov/data/atbd/atbd\\_mod02.pdf](http://modis.gsfc.nasa.gov/data/atbd/atbd_mod02.pdf)]
- ATBD2, 1999: MODIS Normalized Water-Leaving Radiance Algorithm Theoretical Basis Document MOD 18. [Available online at [http://modis.gsfc.nasa.gov/data/atbd/atbd\\_mod17.pdf](http://modis.gsfc.nasa.gov/data/atbd/atbd_mod17.pdf)]
- Bhaskaran, S., Neal, P., Rahman, A., and Mallick, J.: Applications of Satellite Data for Aerosol Optical Depth (AOD) Retrievals and Validation with AERONET Data, *Atmospheric and Climate Sciences*, 01, 61-67, 2011, doi: 10.4236/acs.2011.12007
- Bréon, F., Vermeulen, A., and Descloitres, J.: An evaluation of satellite aerosol products against sunphotometer measurements, *Remote Sens. Environ.*, doi:10.1016/j.rse.2011.06.017, 2011.
- Brunke, M., Wang, Z., Zeng, X., et al.: An Assessment of the Uncertainties in Ocean Surface Turbulent Fluxes in 11 Reanalysis, Satellite-Derived, and Combined Global Datasets, *J. Climate*, 24, 5469-5493, 2011, doi: 10.1175/2011JCLI4223.1

- Carder, K. L., Chen, F. R., Cannizzaro, J. P., Campbell, J. W., Mitchell, B. G., Performance of the MODIS semi-analytical ocean color algorithm for chlorophyll-*a*, *Advances in Space Research*, 33, 1152-1159, 2003.
- Charlson, R., Shwartz, S., Hales, J., et al.: Climate Forcing by Anthropogenic Aerosols, *Science*, 255, 423-430, 1992.
- Chatterjee, A., Michalak, A. M., Kahn, R., et al.: A geostatistical data fusion technique for merging remote sensing and ground-based observations of aerosol optical thickness, *J. Geophys. Res.*, 115, 1-12, 2010, doi: 10.1029/2009JD013765
- Cox, C., and Munk, W.: Statistics of the sea surface derived from sun glitter, *Journal Maritime Science*, 13, 198-227, 1954.
- Drury, E., D. J. Jacob, J. Wang, R. J. D. Spurr, and K. Chance: Improved algorithm for MODIS satellite retrievals of aerosol optical depths over land, *J. Geophys. Res.*, 113, D16204, 2008, doi:16210.11029/12007JD009573
- Eck, T., Holben, B., Reid, J., and Dubovik, O.: Wavelength dependence of the optical depth of biomass burning, urban, and desert dust aerosols, *J. Geophys. Res.*, 104, 1999.
- Esaias, W. E., Abbott, M. R., Barton, I., Brown, O. B., Campbell, J. W., Carder, K. L., Clark, D. K., Evans, R. H., Hoge, F. E., Gordon, H. R., Balch, W. M., Letelier, R., Minnett, P. J.: An overview of MODIS capabilities for ocean science observations, *IEEE Trans. Geosci. Remote Sens.*, 36, 1250-1265, 1998.
- Gordon, H. R. and D. K. Clark: Clear water radiances for atmospheric correction of coastal zone color scanner imagery, *Applied Optics*, 20, 4175-4180, 1981.
- Gordon, H. R., and M. Wang: Retrieval of water-leaving radiance and aerosol optical thickness over the oceans with SeaWiFS: a preliminary algorithm, *Applied Optics*, 33, 443-452, 1994.

- Gordon, H. R.: Atmospheric correction of ocean color imagery in the Earth Observing System era, *J. Geophys. Res.*, 102(102), 17,081-17,106, 1997.
- Hoff, R., and S. A. Christopher: Remote sensing of particulate matter air pollution from space: have we reached the promised land?, *J. Air&Waste Manage. Assoc.*, 59, 642-675, 2009.
- Holben, B., Eck, T., Slutsker, I., et al.: AERONET—A Federated Instrument Network and Data Archive for Aerosol Characterization, *Remote Sens. Environ.*, 66, 1-16, 1998.
- Holt, E., and J. Wang, Trends of wind speed at wind turbine height of 80 m over the contiguous United States using the North American Regional Reanalysis (NARR), *J. Appl. Meteor. Climatol.*, 2012, in press.
- Hsu, N. C., Gautam, R., Sayer, A. M., Bettenhausen, C., Li, C., Jeong, M. J., Tsay, S.-C., and Holben, B. N.: Global and regional trends of aerosol optical depth over land and ocean using SeaWiFS measurements from 1997 to 2010, *Atmos. Chem. Phys. Discuss.*, 12, 8465-8501, doi:10.5194/acpd-12-8465-2012, 2012.
- Hyer, E. J., Reid, J. S., and Zhang, J.: An over-land aerosol optical depth data set for data assimilation by filtering, correction, and aggregation of MODIS Collection 5 optical depth retrievals, *Atmos. Meas. Tech.*, 4, 379-408, 2011, doi:16210.11029/12007JD009573
- Ichoku, C., Chu, D., Mattoo, S., et al.: A spatio-temporal approach for global validation and analysis of MODIS aerosol products, *Geophys. Res. Lett.*, 29, 1-4, 2002, doi: 10.1029/2001GL013206
- Kahn, R. A.: Multiangle Imaging Spectroradiometer (MISR) global aerosol optical depth validation based on 2 years of coincident Aerosol Robotic Network (AERONET) observations, *J. Geophys. Res.*, 110, 1-16, 2005, doi: 10.1029/2004JD004706

Kahn, R., Garay, M., Nelson, D., et al.: Satellite-derived aerosol optical depth over dark water from MISR and MODIS: Comparisons with AERONET and implications for climatological studies, *J. Geophys. Res.*, 112, 2007, doi: 10.1029/2006JD008175

Kahn, R., Garay, M., Nelson, D., et al.: Response to “Toward unified satellite climatology of aerosol properties. 3. MODIS versus MISR versus AERONET,” *J. Quant. Spectrosc. Ra.*, 112, 901-909, 2011, doi: 10.1016/j.jqsrt.2010.11.001

Kaufman, Y., Tanri, D., Remer, L., et al.: Operational remote sensing of tropospheric aerosol over land from EOS moderate resolution imaging Spectroradiometer, *J. Geophys. Res.*, 102, 17051-17067, 1997.

Kennedy A., Dong, X., Xi, B., et al.: A Comparison of MERRA and NARR Reanalyses with the DOE ARM SGP Data, *J. Climate*, 24, 4541-4557, 2011, doi: 10.1175/2011JCLI3978.1

Kinne S.: Monthly averages of aerosol properties: A global comparison among models, satellite data, and AERONET ground data, *J. Geophys. Res.*, 108, 2003, doi: 10.1029/2001JD001253

Kleidman, R., Smirnov, A., Levy, R., et al.: Evaluation and Wind Speed Dependence of MODIS Aerosol Retrievals Over Open Ocean, *IEEE T. Geosci. Remote*, 50, 429-435, 2012, doi: 10.1109/TGRS.2011.2162073

Koepke, P.: Effective reflectance of oceanic whitecaps, *Appl. Optics*, 23, 1816-1824, 1984.

Lavagnini, A., Sempreviva, A., Transerici, C., et al.: Offshore wind climatology over the Mediterranean basin, *Wind Energy*, November, 251-266, 2005, doi: 10.1002/we.169

Levy, R., Remer, L., Martins, J., et al.: Evaluation of the MODIS Aerosol Retrievals over Ocean and Land during CLAMS, *J. Atmos. Sci.*, 62, 974-992, 2005, doi: 10.1175/JAS3391.1

Levy, R., Remer, L., and Dubovik, O.: Global aerosol optical properties and application to Moderate Resolution Imaging Spectroradiometer aerosol retrieval over land, *J. Geophys. Res.*, 112, 1-15, 2007a, doi: 10.1029/2006JD007815

Levy, R., Remer, L., Mattoo, S., et al.: Second-generation operational algorithm: Retrieval of aerosol properties over land from inversion of Moderate Resolution Imaging Spectroradiometer spectral reflectance, *J. Geophys. Res.*, 112, 1-21, 2007b, doi: 10.1029/2006JD007811

Levy, R., Remer, L., Kleidman, R., et al.: Global evaluation of the Collection 5 MODIS dark-target aerosol products over land, *Atmos. Chem. Phys.*, 10, 10399-10420, 2010, doi: 10.5194/acp-10-10399-2010

Li, R.-R., Y. Kaufman, B.-C. Gao, and C. Davis: Remote sensing of suspended sediments and shallow coastal waters, *IEEE Trans. Geosci. Remote Sens.*, 41, 559-566, 2003.

Martín, M., Cremades, L., and Santabàrbara, J.: Analysis and modeling of time series of surface wind speed and direction, *Int. J. Climatol.*, 19, 197-209, 1999.

Mi, W., Li, Z., Xia, X., et al.: Evaluation of the Moderate Resolution Imaging Spectroradiometer aerosol products at two Aerosol Robotic Network stations in China, *J. Geophys. Res.*, 112, 1-14, 2007, doi: 10.1029/2007JD008474

Mishchenko, M., and Geogdzhayev, I.: Satellite remote sensing reveals regional tropospheric aerosol trends, *Opt. Express*, 15, 7423-38, 2007.

Mishchenko, M., Geogdzhayev, I., Rossow, W., et al.: Long-Term Satellite Record Reveals Likely Recent Aerosol Trend, *Science*, 315, 1534, 2007, doi: 10.1126/science.1136709

Myhre, Gunnar: Consistency Between Satellite-Derived and Modeled Estimates of the Direct Aerosol Effect, *Science*, 324, 187-190, 2009, doi: 10.1126/science.1174461

- O'Neill, N. T., Ignatov, A., Holben, B. N., and Eck, T. F.: The lognormal distribution as a reference for reporting aerosol optical depth statistics; Empirical tests using multi-year, multi-site AERONET sunphotometer data, *Geophys. Res. Lett.*, 27, 2000, doi: 10.1029/2000GL011581
- Petrenko, M., Ichoku, C., and Leptoukh, G.: Multi-sensor Aerosol Products Sampling System (MAPSS), *Atmos. Meas. Tech.*, 5, 913-926, 2012, doi : 10.5194/amt-5-913-2012
- Remer, L., Kaufman, Y., Tanre, D., et al.: The MODIS Aerosol Algorithms, Products, and Validation. *J. Atmos. Sci.*, 62, 947-973, 2005, doi: 10.1175/JAS3385.1
- Remer, L., Kleidman, R., Levy, R., et al.: Global aerosol climatology from the MODIS satellite sensors, *J. Geophys. Res.*, 113, 1-18, 2008, doi: 10.1029/2007JD009661
- Rienecker, M., Suarez, M., Gelaro, R., et al.: MERRA - NASA's Modern-Era Retrospective Analysis for Research and Applications, *J. Climate*, 24, 3624-3648, 2011, doi: 10.1175/JCLI-D-11-00015.1
- Samet, J., Zegar, S., Dominici, F., et al.: The National Morbidity, Mortality, And Air Pollution Study Part II: Morbidity and Mortality from Air Pollution in the United States, *Health Effects Institute*, 94, 2000.
- Shi, Y., Zhang, J., Reid, R., et al.: An analysis of the collection 5 MODIS over-ocean aerosol optical depth product for its implication in aerosol assimilation, *Atmos. Chem. Phys.*, 11, 557-565, 2011, doi: 10.5194/acp-11-557-2011
- Smirnov, A., Holben, B. N., Eck, T. F., Dubovik, O., and Slutsker, I.: Cloud-Screening and quality control algorithms for the AERONET database, *Remote Sens. Environ.*, 73, 337-349, 2000, doi: 10.1016/S0034-4257(00)00109-7

- Smirnov, A., Holben, B., Giles, D., et al.: Maritime Aerosol Network as a component of AERONET – first results and comparison with global aerosol models and satellite retrievals, *Atmos. Meas. Tech. Discussions*, 4, 1-32, 2011, doi: 10.5194/amtd-4-1-2011
- Taylor, K. E.: Summarizing multiple aspects of model performance in a single diagram, *J. Geophys. Res.*, 106, 7183-7192, 2001, doi: 10.1029/2000JD900719
- Tibbetts, J.: Coastal Cities: Living on the Edge, *Environ. Health Persp.*, 110, 674-681, 2002.
- Wang, J., X. Xu, R. Spurr, Y. Wang, and E. Drury: Improved algorithm for MODIS satellite retrievals of aerosol optical thickness over land in dusty atmosphere: Implications for air quality monitoring in China, *Remote Sens. Environ.*, 114, 2575-2583, 2010.
- Wilks, Daniel S.: *Frequentist Statistical Inference*, in *Statistical Methods in the Atmospheric Sciences*, Third Edition, Academic Press, San Diego, California, 2011.
- Yu, H., et al.: A review of measurement-based assessment of aerosol direct radiative effect and forcing, *Atmos. Chem. Phys.*, 6, 613-666, 2006.
- Zhang, J., and Reid, J.: MODIS aerosol product analysis for data assimilation: Assessment of over-ocean level 2 aerosol optical thickness retrievals, *J. Geophys. Res.*, 111, 1-17, 2006, doi: 10.1029/2005JD006898
- Zhang, J., and Reid, J.: A decadal regional and global trend analysis of the aerosol optical depth using a data-assimilation grade over-water MODIS and Level 2 MISR aerosol products, *Atmos. Chem. Phys.*, 10, 18879-18917, 2010, doi: 10.5194/acp-10-10949-2010
- Zhao, X.-P. T., Heidinger, A., and Knapp, K.: Long-term trends of zonally averaged aerosol optical thickness observed from operational satellite AVHRR instrument, *Meteorol. Appl.*, 18: 440–445, 2011, doi: 10.1002/met.235

**Table 1.** MODIS AOD mean bias over the full data record (2002-2011) for all AERONET coastal stations. 62 coastal AERONET sites were identified and the results are an average of all the sites. Each of the MODIS aerosol algorithms is shown with the recommended quality control except for the Land\_And\_Ocean product which is shown without any quality control (default MODIS product) and the results of our quality control technique described in Section 4. Bias results are separated into Low AOD and High AOD events as classified by AERONET measurements with the cutoff at 0.25.

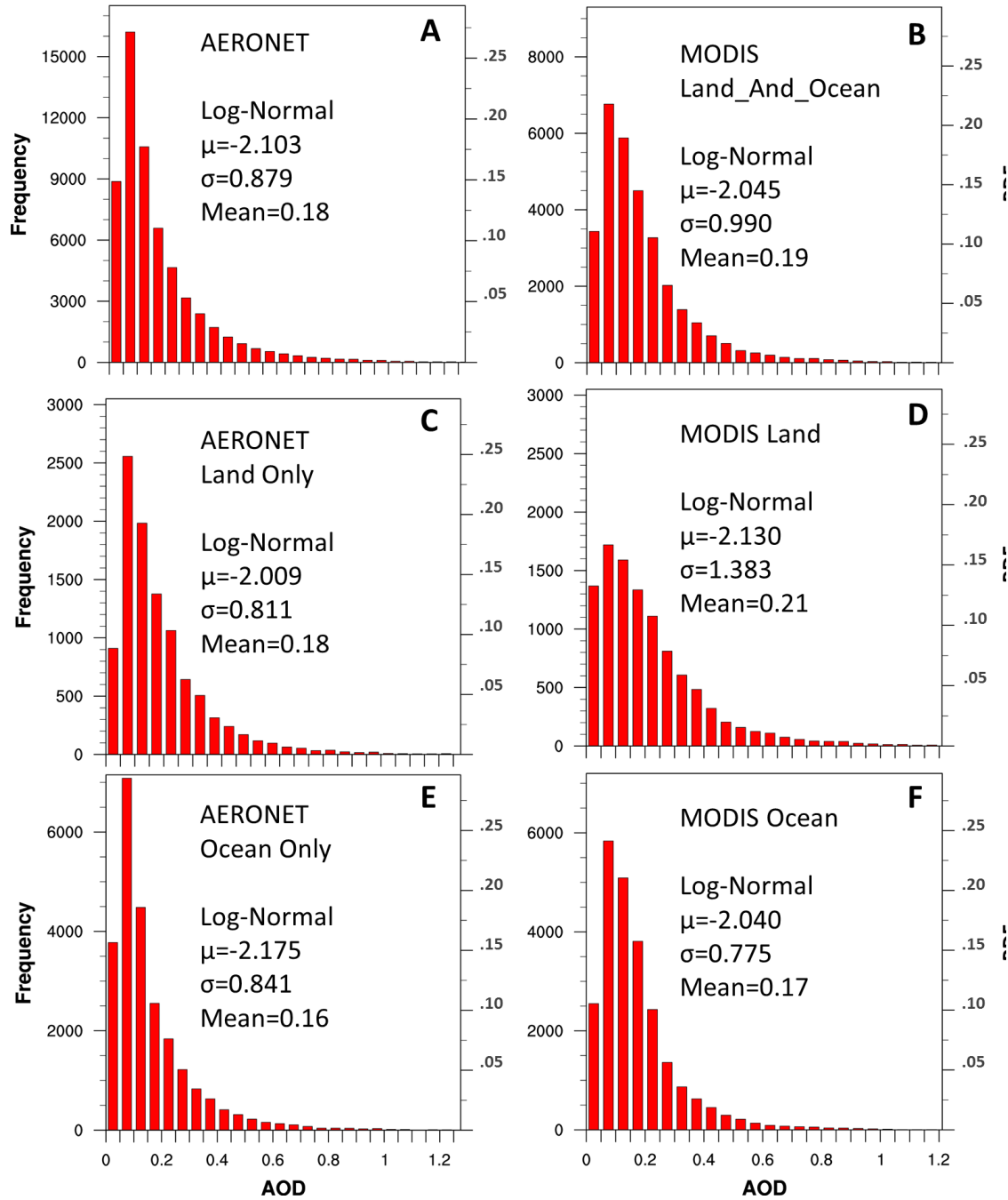
<b>All Coastal Sites</b>	<b>Land Algorithm</b>	<b>Ocean Algorithm</b>	<b>Land_And_Ocean</b>	
	<b>QA Filtered</b>	<b>QA Filtered</b>	<b>No Filter</b>	<b>QA Filtered</b>
<b>Total Bias</b>	<b>0.026</b>	<b>0.006</b>	<b>0.029</b>	<b>0.019</b>
<b>Low AOD Bias</b>	<b>0.024</b>	<b>0.021</b>	<b>0.033</b>	<b>0.024</b>
<b>High AOD Bias</b>	<b>0.026</b>	<b>-0.029</b>	<b>0.026</b>	<b>0.010</b>

**Table 2.** MODIS AOD bias with respect to AERONET AOD for both coastal and open ocean sites. The bias is listed for three categories on how MODIS AOD is used in the evaluation. The first is filtering of data with quality control flag; the second builds upon the first but also removes MODIS AOD data with cloud fraction larger than 80%; the third is the same as second except the threshold for cloud fraction is now decreased to 70%. The number of AOD retrievals used in the different analyses (last row in Table 2) is also shown to display the reduction in data size associated with each category. In each category, bias is further analyzed in terms of low AOD conditions (AOD < 0.25) and high AOD conditions. In addition, the relative percent change of bias due to the filtering of data with cloud fraction is shown in in parentheses, negative percentages indicate an increase in bias. See text for further details.

<b>MODIS Cloud Contamination</b>	<b>Normal QA</b>		<b>80% Threshold</b>		<b>70% Threshold</b>	
	<b>Coastal</b>	<b>Open Ocean</b>	<b>Coastal</b>	<b>Open Ocean</b>	<b>Coastal</b>	<b>Open Ocean</b>
<b>Total Bias</b>	<b>0.006</b>	<b>0.012</b>	<b>0.002 (67%)</b>	<b>0.008 (33%)</b>	<b>0.000 (100%)</b>	<b>0.005 (58%)</b>
<b>Low AOD Bias</b>	<b>0.021</b>	<b>0.018</b>	<b>0.018 (14%)</b>	<b>0.013 (28%)</b>	<b>0.016 (24%)</b>	<b>0.011 (39%)</b>
<b>High AOD Bias</b>	<b>-0.029</b>	<b>-0.022</b>	<b>-0.035(-21%)</b>	<b>-0.026(-18%)</b>	<b>-0.035(-21%)</b>	<b>-0.027(-23%)</b>
<b>Number of Retrievals</b>	<b>18,001</b>	<b>4,190</b>	<b>17,104</b>	<b>3,441</b>	<b>15,768</b>	<b>3,118</b>

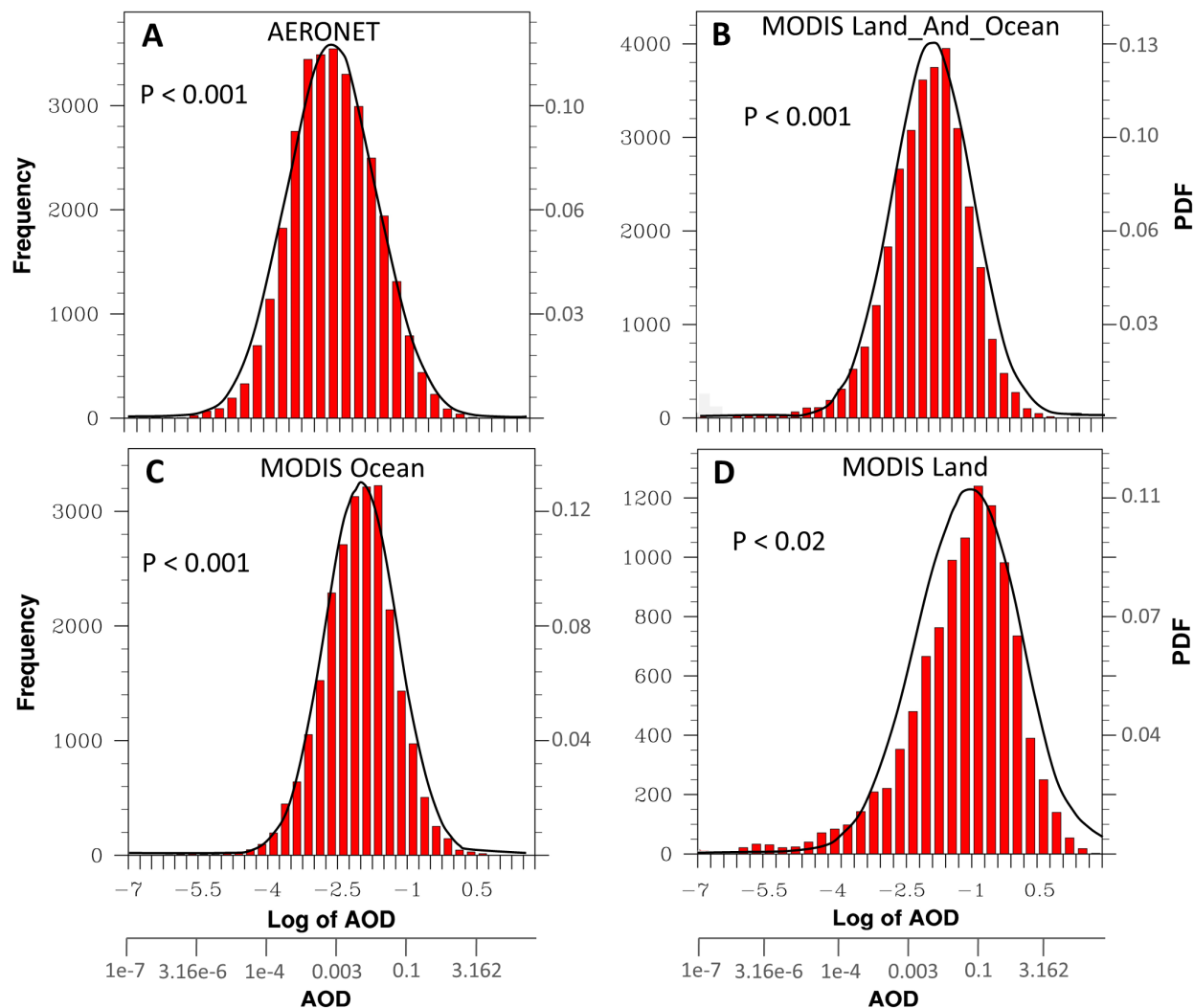
**Table 3.** Regression statistics for the MODIS AOD products with respect to AERONET. Data span 2002-2011.

Regression Statistics	Land			Ocean			Land_And_Ocean No QA			Land_And_Ocean With QA		
	Coastal	Non-Coastal	Global	Coastal	Non-Coastal	Global	Coastal	Non-Coastal	Global	Coastal	Non-Coastal	Global
<b>R<sup>2</sup></b>	<b>0.795</b>	<b>0.795</b>	<b>0.793</b>	<b>0.804</b>	<b>0.854</b>	<b>0.809</b>	<b>0.753</b>	<b>0.73</b>	<b>0.737</b>	<b>0.818</b>	<b>0.801</b>	<b>0.804</b>
<b>Slope</b>	<b>1.027</b>	<b>0.971</b>	<b>0.979</b>	<b>0.863</b>	<b>1.115</b>	<b>0.913</b>	<b>0.948</b>	<b>0.968</b>	<b>0.962</b>	<b>0.933</b>	<b>0.982</b>	<b>0.964</b>
<b>Intercept</b>	<b>0.016</b>	<b>0.004</b>	<b>0.008</b>	<b>0.034</b>	<b>-0.001</b>	<b>0.028</b>	<b>0.037</b>	<b>0.026</b>	<b>0.03</b>	<b>0.029</b>	<b>0.003</b>	<b>0.014</b>



1

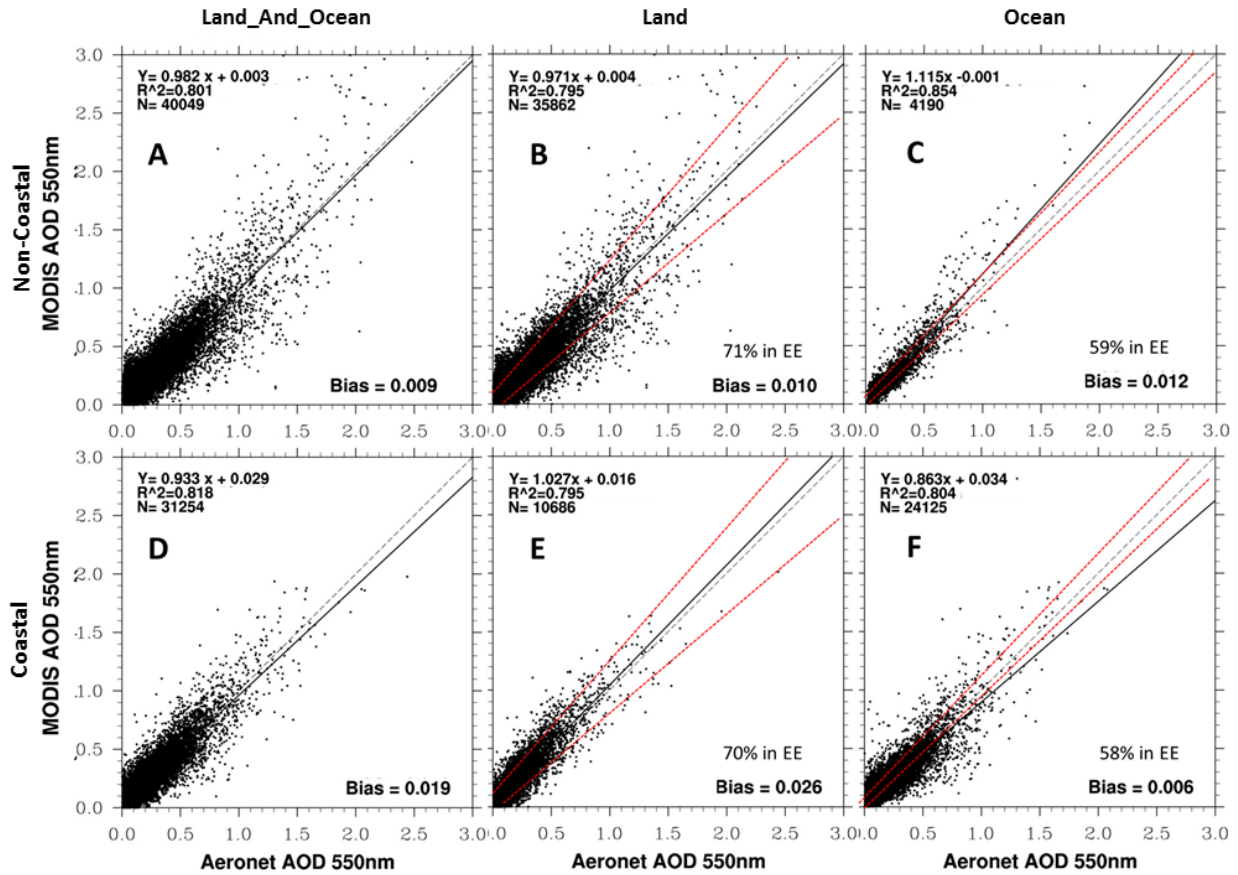
2 **Figure 1.** Frequency (left vertical axis) and PDFs (right vertical axis) of coastal AODs in 20  
3 2011. Plots are derived from AODs at 62 coastal AERONET sites and collocated MODIS  
4 retrievals over those sites.  $\mu$  is the log-normal location parameter and  $\sigma$  is the log-normal sc  
5 parameter, and the mean is the average AOD over the whole time period. (A) – (E) respecti  
6 show quality assured and quality flag filtered frequency of AERONET AODs, MODIS  
7 Land\_And\_Ocean AODs, AERONET AODs only where a paired MODIS AOD from the L  
8 algorithm exists, MODIS AOD from Land algorithm, AERONET AODs only where a pair  
9 MODIS AOD from the Ocean algorithm exists, and MODIS AODs from Ocean algorithm.



11

12 **Figure 2.** Frequency (left vertical axis) and PDFs (right vertical axis) of the coastal AODs from  
 13 (A) AERONET, (B) MODIS Land\_And\_Ocean, (C) MODIS Ocean algorithm, and (D) MODIS  
 14 Land algorithm. All MODIS AODs are filtered with quality flag for the record of 2002-2011.  
 15 The p-values indicate statistical significance of fit between frequency distributions derived from  
 16 the lognormal PDFs (with parameters correspondingly shown in Figure 1) and actual frequency  
 17 distribution (e.g., the bars in red). See text for details. (A) shows only those AERONET AODs  
 18 that correspond to a valid MODIS AOD retrieval.

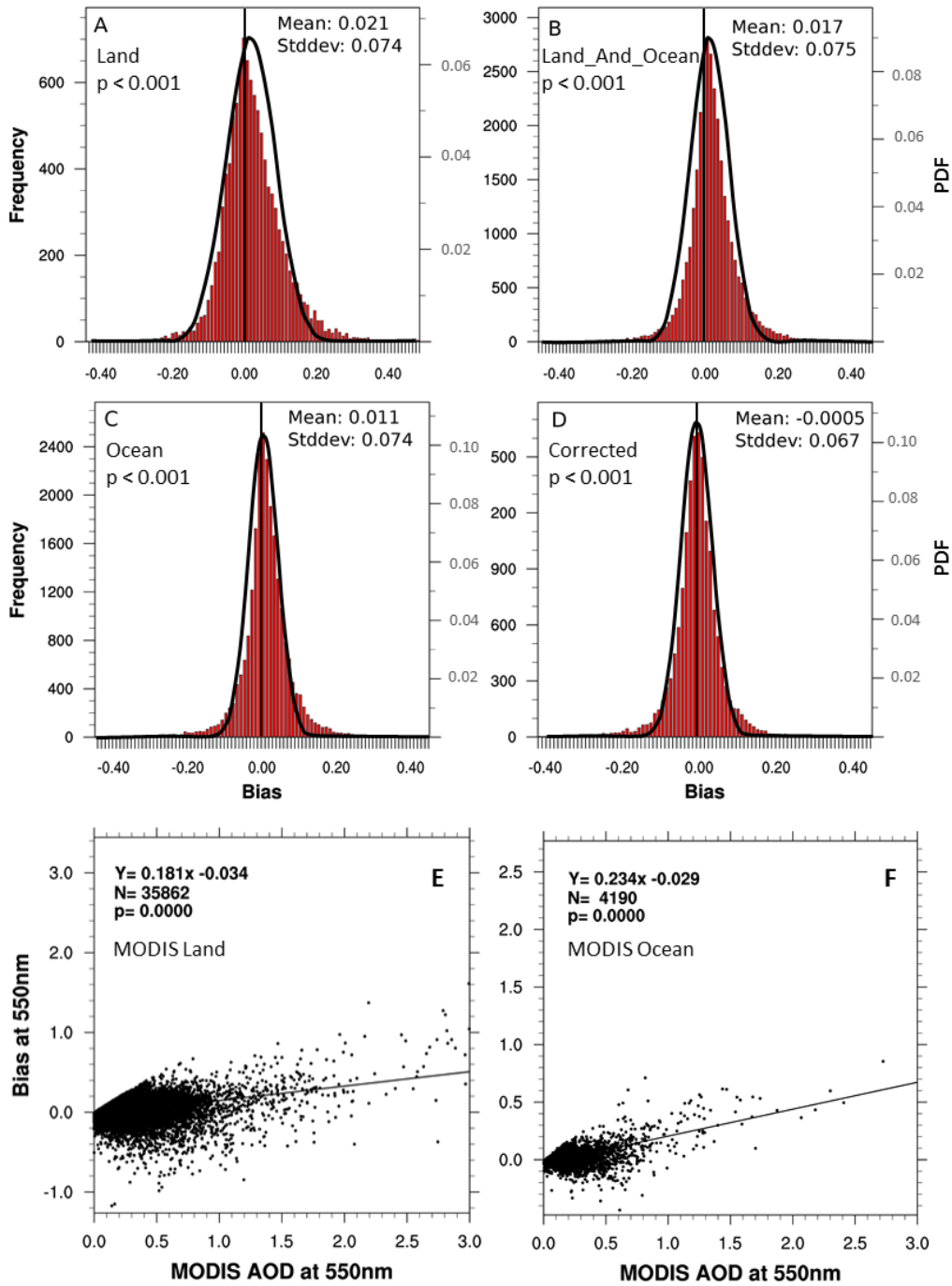
19



20

21 **Figure 3.** Scatter plot of AERONET AOD (x-axis) and the quality flag filtered MODIS AOD (y-  
 22 axis) for 2002-2011. In (A), (B), and (C), AODs in y-axis are respectively derived from MODIS  
 23 Land\_And\_Ocean, Land, and Ocean products over the non-coastal AERONET stations. (D) (E)  
 24 and (F) are respectively the same as (A), (B), and (C) but over the coastal AERONET stations. In  
 25 each scatter plot, also shown is the correlation coefficient ( $R^2$ ), mean bias, the number of  
 26 MODIS-AERONET collocated data points (N), and the best-fit linear regression equation (solid  
 27 black line), the 1:1 line (dashed black line), and the expected error envelope (red dashed line) for  
 28 MODIS AOD explained in Section 3.2.

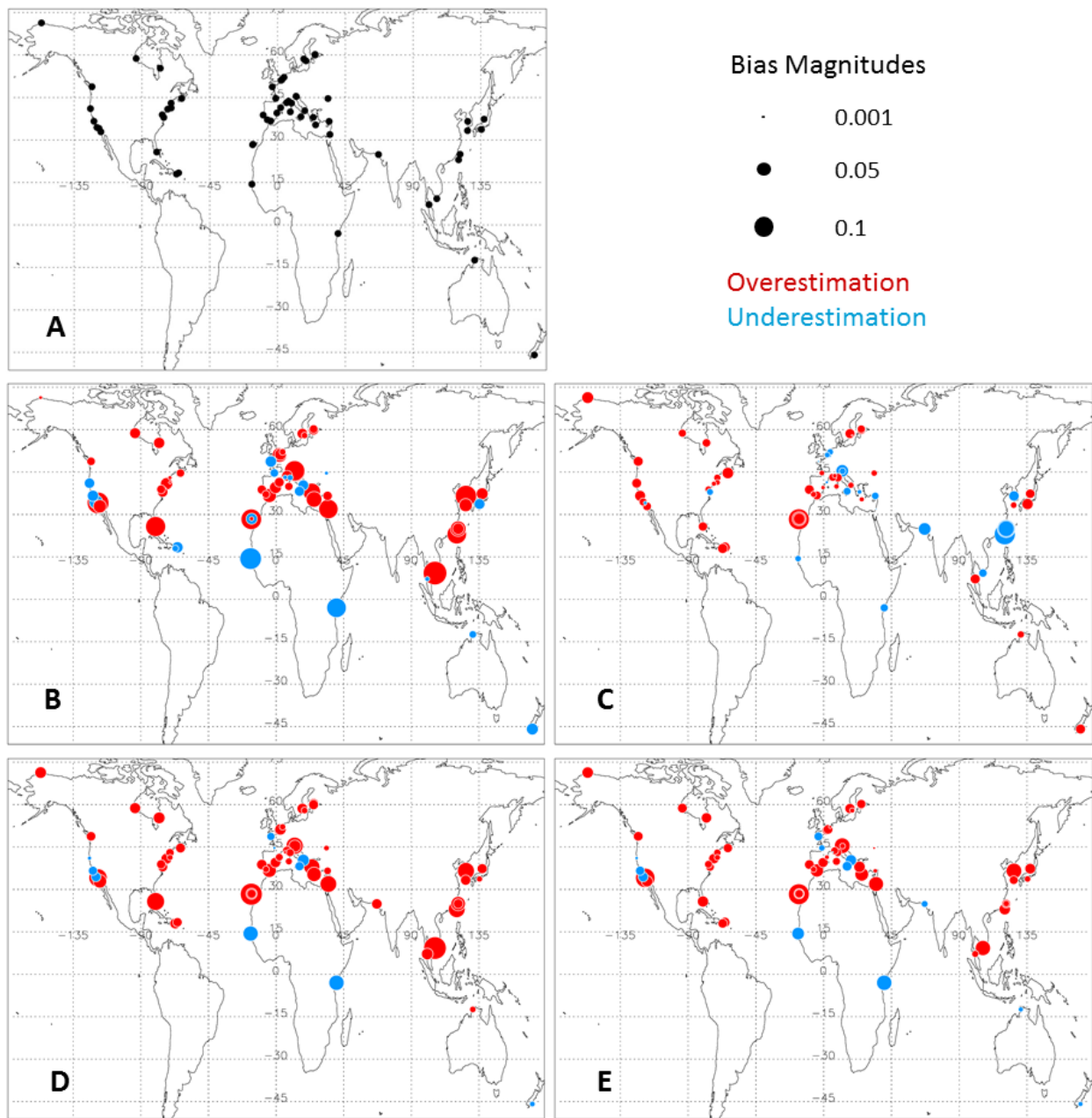
29



30

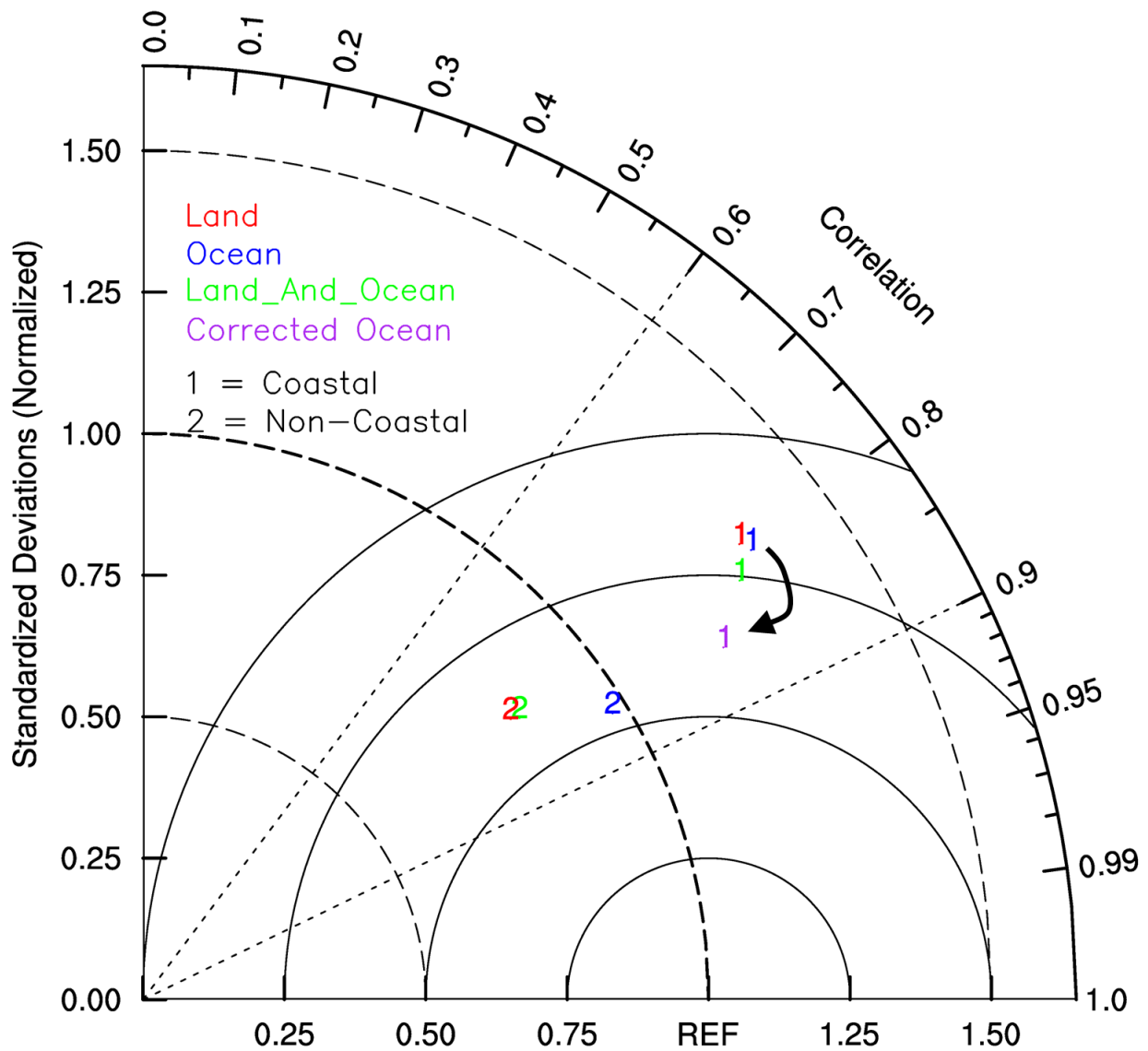
31 **Figure 4.** Frequency (left y-axis) and PDFs (right y-axis) of MODIS AOD biases from the (A)  
 32 Land algorithm, (B) Land\_And\_Ocean product, (C) Ocean algorithm, and (D) the corrected  
 33 Ocean algorithm. Data are for all coastal AERONET sites in 2002-2011. The green and black  
 34 thick lines respectively show the zero bias and mean bias for each panel.

35



36

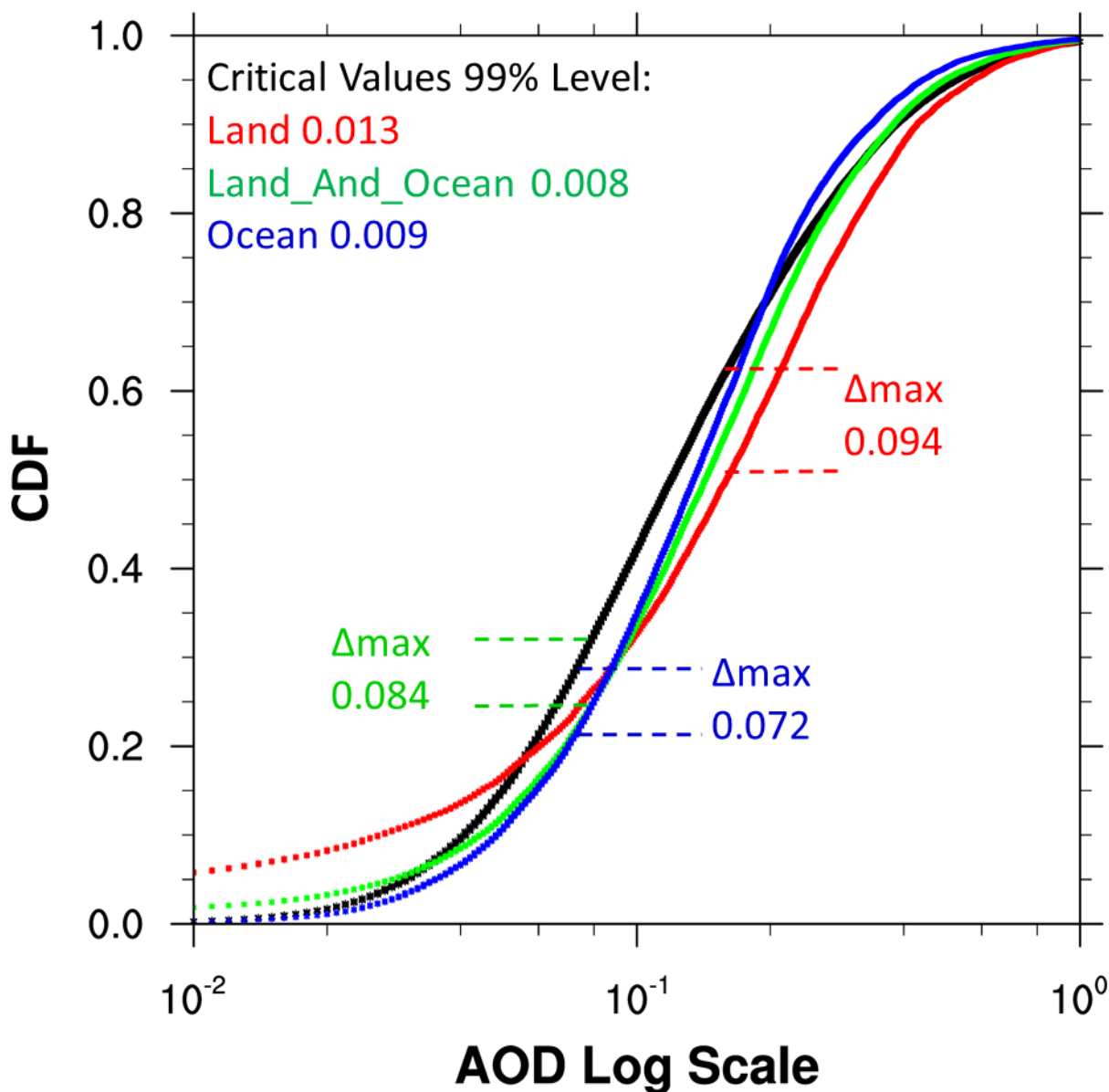
37 **Figure 5.** (A) Map of the location of all 62 coastal AERONET sites; Also shown are the maps of  
 38 MODIS AOD bias (with respect to AERONET AOD) at each of these coastal sites respectively  
 39 for: (B) MODIS Land AODs product filtered with quality flag, (C) MODIS Ocean AODs  
 40 product filtered with quality flag; (D) MODIS Land\_And\_Ocean AODs without any quality  
 41 filtering; (E) MODIS Land\_And\_Ocean AODs after using the method described in the Section 4  
 42 for quality filtering. Bias calculations are based on ~9 years (2002-2011) of collocated MODIS  
 43 and AERONET AOD data. Blue indicates an underestimation (e.g., negative bias) in MODIS  
 44 AOD and red indicates overestimation (positive bias). Common legend for (B)-(E) is shown on  
 45 the left of panel (A).



47

48 **Figure 6.** Taylor diagram comparing ~2002-2011 quality flag filtered MODIS AOD retrievals  
 49 and AERONET AOD observations. Coastal MODIS AOD retrievals are listed with a 1 and Non-  
 50 Coastal AODs are shown with a 2. The MODIS Ocean, Land, Land\_And\_Ocean, and  
 51 empirically corrected Ocean (See Section 5) AODs are represented by blue, red, green, and  
 52 purple respectively. The arrow represents the effect of the empirical correction on the MODIS  
 53 Ocean product.

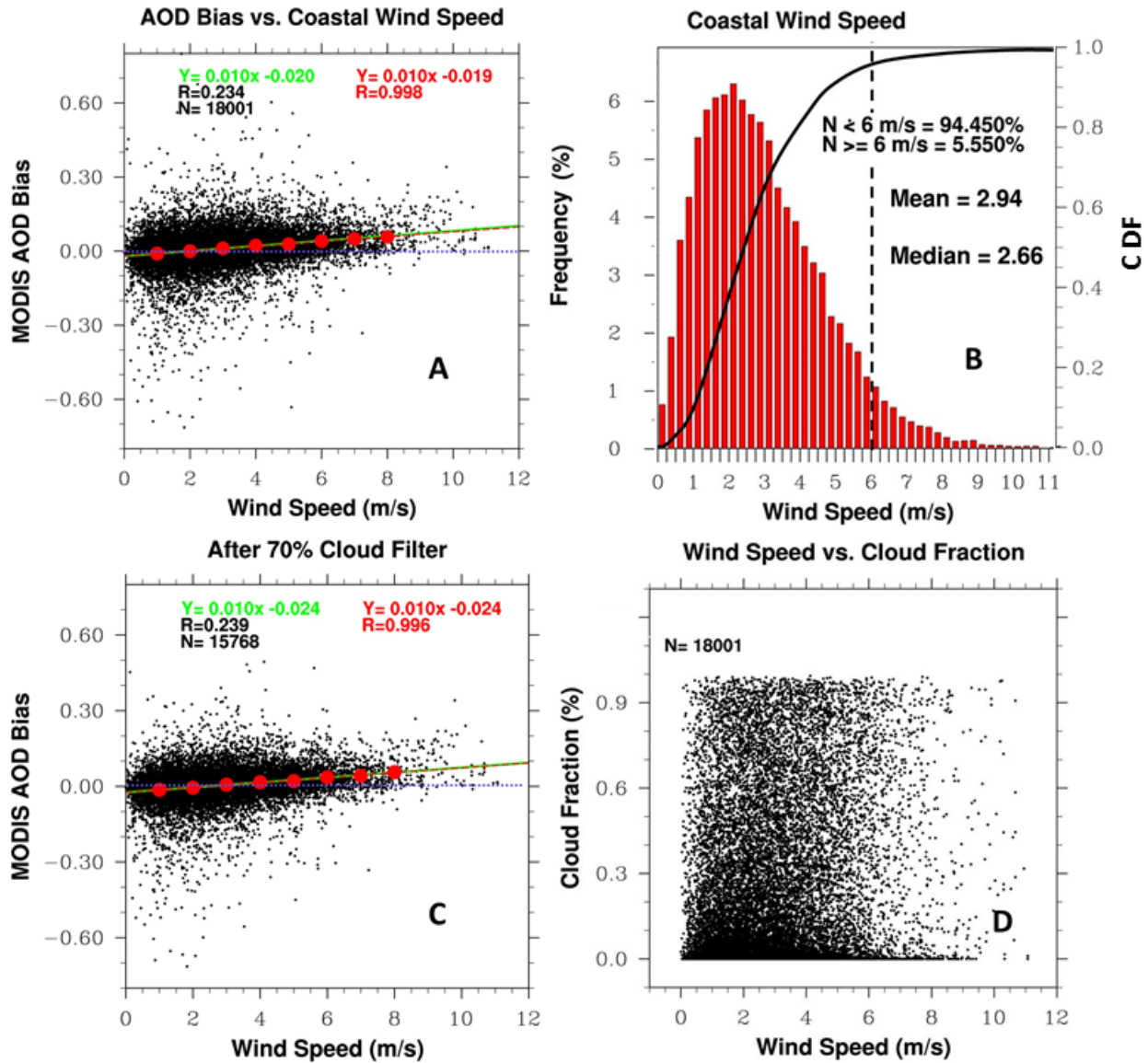
54



55

56 **Figure 7.** Cumulative distribution functions (CDF) of AOD derived from AERONET (black),  
 57 and corresponding paired MODIS AODs derived respectively from MODIS Land (red), Ocean  
 58 (blue), and Land\_And\_Ocean (green) AODs after filtering with quality flag.. Maximum  
 59 differences ( $\Delta_{max}$ ) between the AERONET CDF and MODIS CDFs are shown by two dashed  
 60 horizontal lines and their values are denoted in their respective colors. Statistics are based upon  
 61 MODIS aerosol product in 2002-2011 over coastal regions. Critical values for the K-S test are  
 62 also denoted in the top left of the figure and are described in text (Sections 3.1).

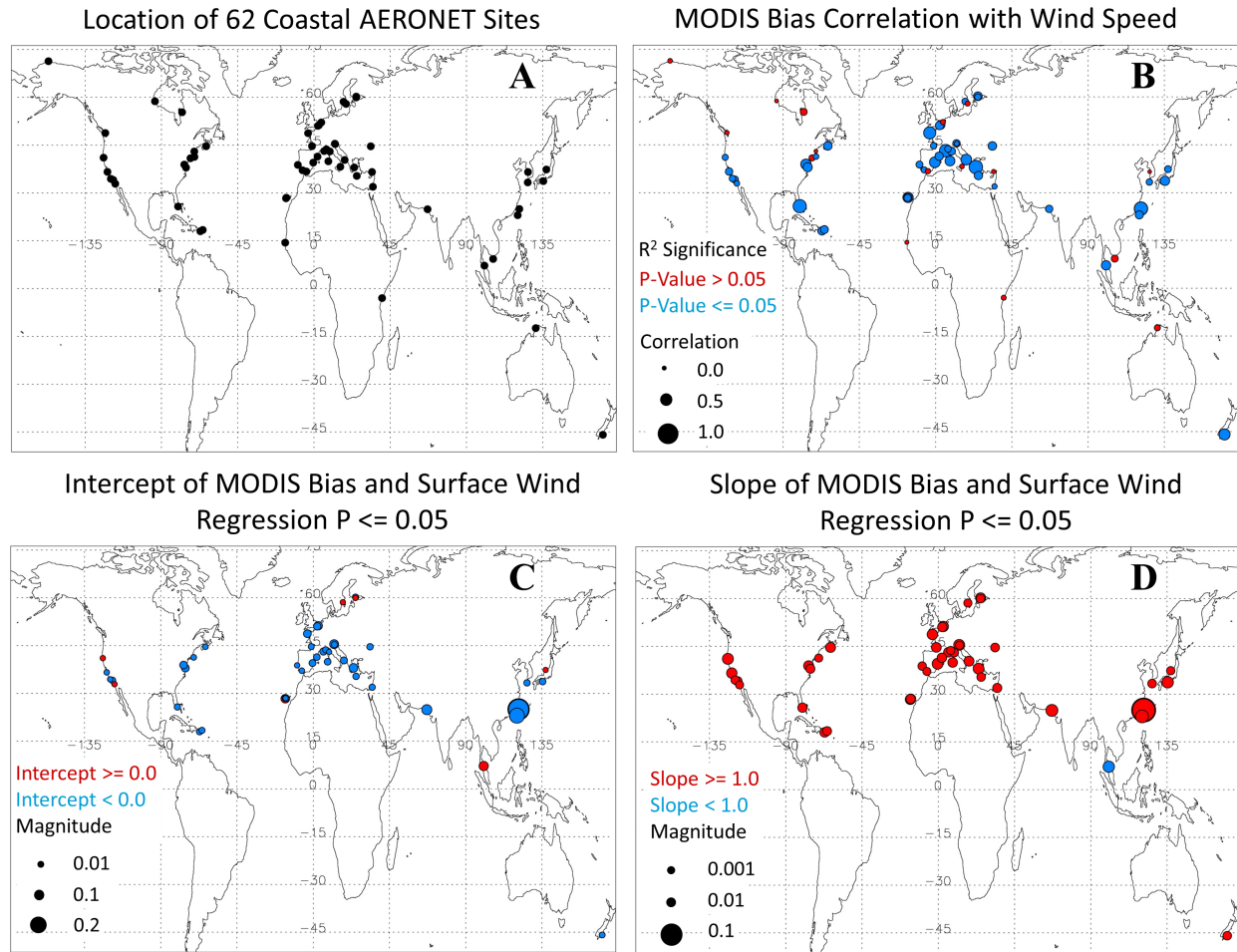
63



65

66 **Figure 8.** (A) Scatter plot of 2 m coastal wind speeds from MERRA (x-axis) and the biases in  
 67 the quality flag filtered AODs. (B) the frequency (left y-axis) and CDF (right y-axis) of coastal  
 68 wind speeds during MODIS overpass times. (C): same as (A) but for the bias of MODIS AOD  
 69 after 70% cloud fraction filter. (D) scatter plot of the wind speed and cloud fraction pairs for  
 70 each AOD retrieval from MODIS Ocean algorithm. The analysis is for all coastal sites (62  
 71 AERONET sites) and for the years ~2002-2011. R is the Pearson linear correlation coefficient, N  
 72 is the number of retrievals and Y is the regression equation. In (A) and (C), red dots show the  
 73 MODIS biases binned to  $1 \text{ ms}^{-1}$  intervals, and their corresponding regression lines and  
 74 correlation are denoted in red as well; the blue dotted line is a reference of zero bias.

75

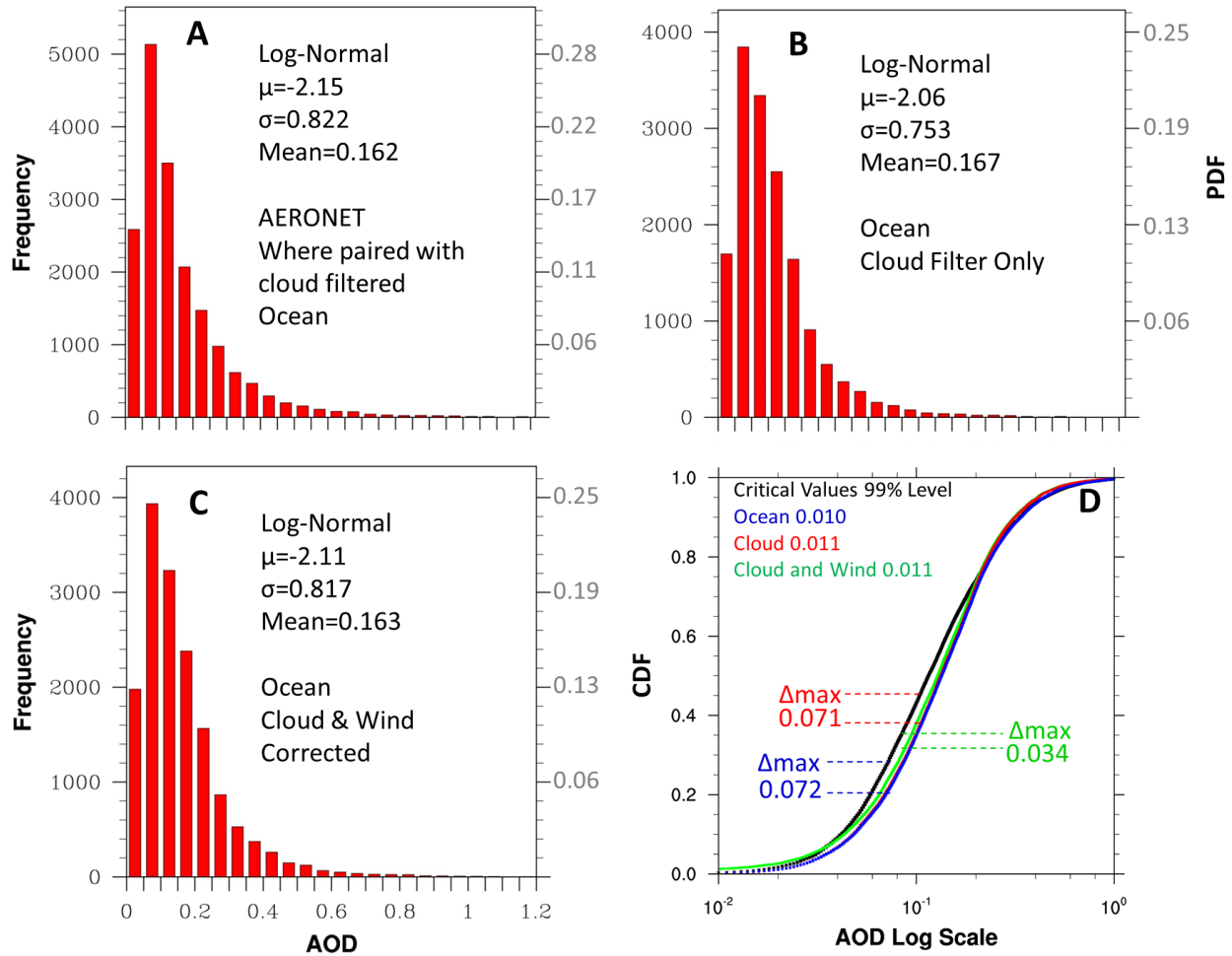


76

77 **Figure 9.** (A) Locations for each coastal AERONET site, (B) the correlation between sea-surface  
 78 wind speed and the biases in quality flag filtered AODs from MODIS Ocean algorithm, (C) and  
 79 (D) respectively show the the y-intercept and slope in the linear regression equation between the  
 80 MODIS AOD biases and wind speed. Blue colors represent statistically significant values in (B)  
 81 and negative intercepts and slopes for (C) and (D), respectively. Red represents statistically  
 82 insignificant values in (B) and positive intercepts and slopes for (C) and (D). Magnitude scales  
 83 are shown by size of the circle, and are provided in each panel for clarity. (C) and (D) show only  
 84 sites with p-value less than or equal to 0.05 (46 out of the possible 62 sites). Results are for date  
 85 record of 2002-2011.

86

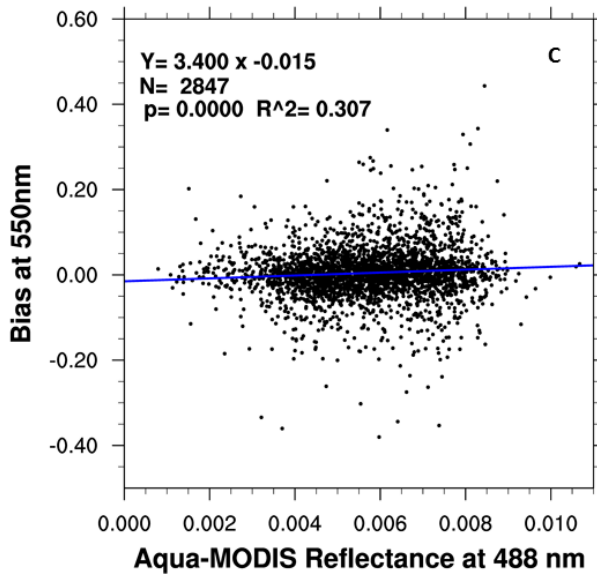
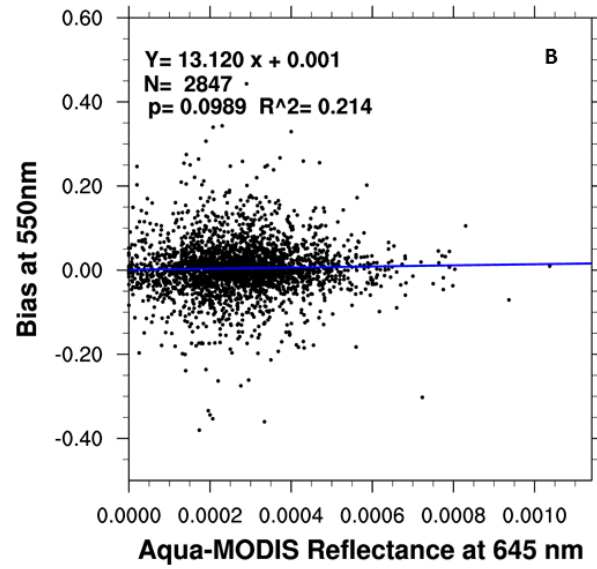
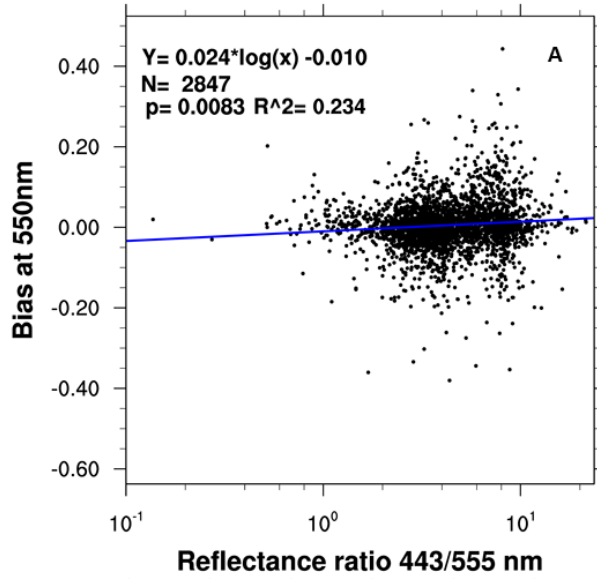
87



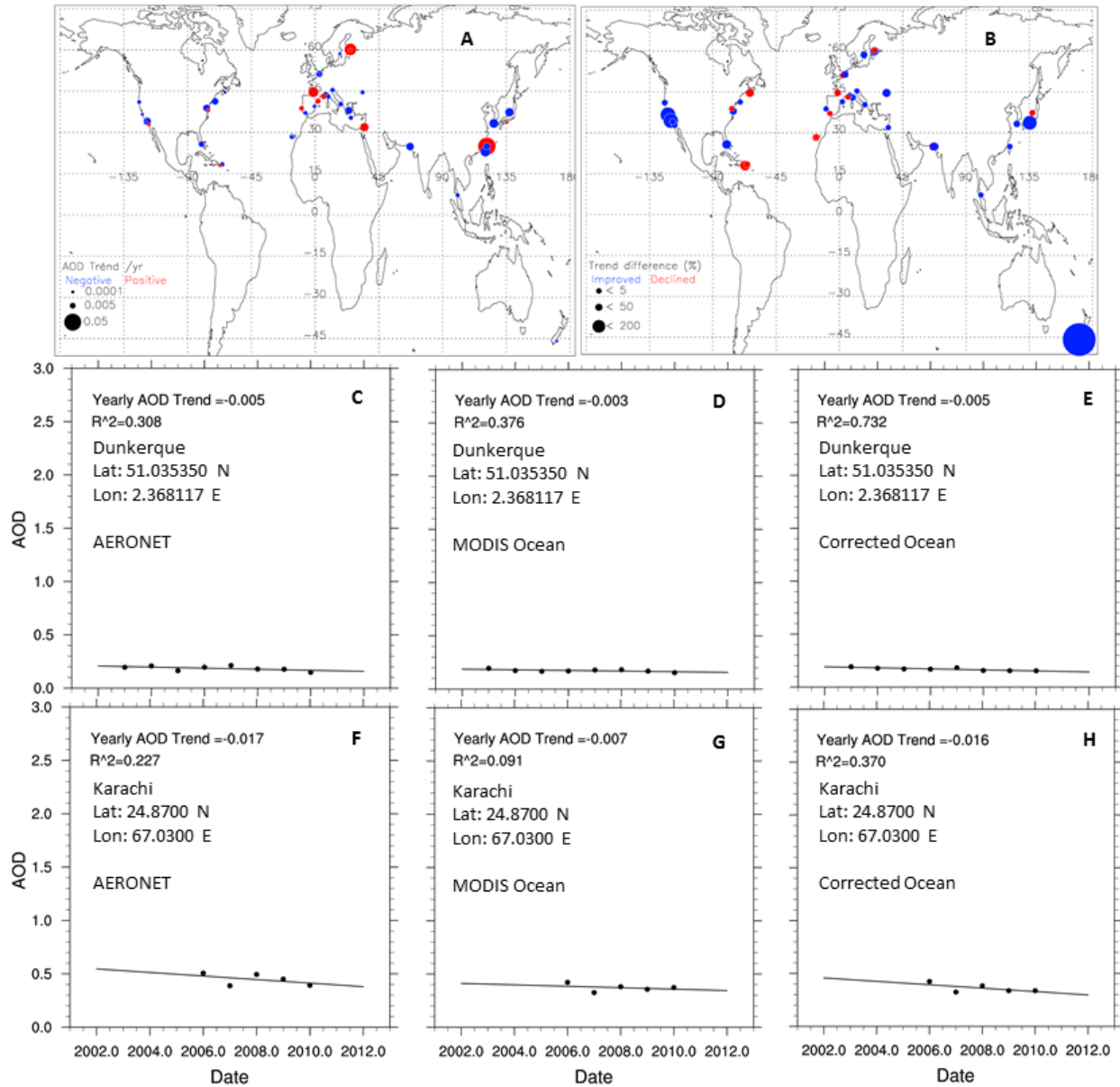
88

89 **Figure 10.** Frequency distribution of quality assured (A) AERONET AOD over coastal regions  
90 that have an MODIS Ocean algorithm collocated retrieval, (B) AOD from MODIS Ocean  
91 algorithm after cloud fraction and quality flag filtering only, (C) AOD from MODIS Ocean  
92 algorithm after cloud fraction filtering (70%), wind speed bias correction, and quality flag  
93 filtering. (D): same as Figure 7 except the cumulative distribution functions (CDF) is derived  
94 from the frequency distributions respectively in (A)-(C) and Figure 2c, and shown  
95 correspondingly as black, red, and blue color respectively.

96



98 **Figure 11.** (A) Scatter plot of the bias for coastal MODIS AOD (retrieved from the Ocean  
99 algorithm) as a function of the ratio of remote-sensing surface reflectance (Rrs) between 443 nm  
100 and 555nm. (B) (C) are the same as (A) except the x-axis shows the Rrs at 645 nm and 488 nm  
101 respectively. See Section 2.1 in the text for details. Also shown in the each panel is the best  
102 linear fit equation, the statistical significance (p value) of the fit, and number of data points (N).



103

104 **Figure 12.** (A) Spatial distribution of the trend of annual AOD at different AERONET sites that  
 105 have at least 6 years of data during 2002-2010. Blue indicates negative AOD trends while red  
 106 indicates positive AOD trends. The size of the circle is relatively proportional to the absolute  
 107 value of the trend. (B) The relative difference (in %) between annual AOD trends computed with  
 108 MODIS before and after the empirical correction, defined as the  $(|Trend\_modis\_corrected| - |Trend\_modis - Trend\_aeronet|) / |Trend\_aeronet|$ ;  
 109 negative value is shown in blue, and indicates that  $Trend\_modis\_corrected$  is closer to  $Trend\_aeronet$  than  $Trend\_modis$ ;  
 110 positive value is shown in red, and indicates that  $Trend\_modis\_corrected$  is further away from  
 111  $Trend\_aeronet$  than  $Trend\_modis$ . See section 5 for details.

113